



**HAL**  
open science

## **pin2 mutant agravitropic root phenotype is conditional and nutrient-sensitive**

Marion Thomas, Alexandre Soriano, Claire O'connor, Amandine Crabos, Philippe Nacry, Megan Thompson, Estelle Hrabak, Fanchon Divol, Benjamin Péret

### ► To cite this version:

Marion Thomas, Alexandre Soriano, Claire O'connor, Amandine Crabos, Philippe Nacry, et al.. pin2 mutant agravitropic root phenotype is conditional and nutrient-sensitive. *Plant Science*, 2023, 329, pp.111606. 10.1016/j.plantsci.2023.111606 . hal-03960045

**HAL Id: hal-03960045**

**<https://hal.inrae.fr/hal-03960045>**

Submitted on 30 Jan 2023

**HAL** is a multi-disciplinary open access archive for the deposit and dissemination of scientific research documents, whether they are published or not. The documents may come from teaching and research institutions in France or abroad, or from public or private research centers.

L'archive ouverte pluridisciplinaire **HAL**, est destinée au dépôt et à la diffusion de documents scientifiques de niveau recherche, publiés ou non, émanant des établissements d'enseignement et de recherche français ou étrangers, des laboratoires publics ou privés.

# 1 ***pin2* mutant agravitropic root phenotype is conditional and nutrient-sensitive**

2 Marion Thomas <sup>a</sup>, Alexandre Soriano <sup>a,1</sup>, Claire O'Connor <sup>a</sup>, Amandine Crabos <sup>a</sup>, Philippe  
3 Nacry <sup>a</sup>, Megan Thompson <sup>b</sup>, Estelle Hrabak <sup>b</sup>, Fanchon Divol <sup>a</sup>, Benjamin Péret <sup>a\*</sup>.

## 4 Affiliations

5 <sup>a</sup> IPSiM, Univ Montpellier, CNRS, INRAE, Institut Agro, Montpellier, France

6 <sup>b</sup> Univ New Hampshire, Durham, USA

7 <sup>1</sup> Present address: AGAP, Univ Montpellier, CIRAD, INRAE, Institut Agro, Montpellier,  
8 France

9

10 \*For correspondence:

11 benjamin.peret@cirs.fr (+ 33 (0) 499612859)

12 Benjamin Péret: 0000-0003-1336-0796

13 Number of items:

14 Word count: 5778

15

## 16 Abstract

17 Plants have the capacity to sense and adapt to environmental factors using the  
18 phytohormone auxin as a major regulator of tropism and development. Among these  
19 responses, gravitropism is essential for plant roots to grow downward in the search for  
20 nutrients and water. We discovered a new mutant allele of the auxin efflux transporter *PIN2*  
21 that revealed that *pin2* agravitropic root mutants are conditional and nutrient-sensitive. We  
22 describe that nutrient composition of the medium, rather than osmolarity, can revert the  
23 agravitropic root phenotype of *pin2*. Indeed, on phosphorus- and nitrogen-deprived media,  
24 the agravitropic root defect was restored independently of primary root growth levels. Slow  
25 and fast auxin responses were evaluated using DR5 and R2D2 probes, respectively, and  
26 revealed a strong modulation by nutrient composition of the culture medium. We evaluated  
27 the role of PIN and AUX auxin transporters and demonstrated that neither PIN3 nor AUX1  
28 are involved in this process. However, we observed the ectopic expression of *PIN1* in the  
29 epidermis in the *pin2* mutant background associated with permissive, but not restrictive,  
30 conditions. This ectopic expression was associated with a restoration of the asymmetric  
31 accumulation of auxin necessary for the reorientation of the root according to gravity. These  
32 observations suggest a strong regulation of auxin distribution by nutrients availability, directly  
33 impacting root's ability to drive their gravitropic response.

34

35 Key words: Polar auxin transport, PIN1, PIN2, gravitropism, nutrients, conditional phenotype

36

37 1. Introduction

38 Gravitropism is essential to monitor gravity and allow roots to anchor themselves in the soil,  
39 where they navigate heterogeneous environments to uptake water and nutrients. The key  
40 phytohormone auxin controls many stages of plant development and tropism, including  
41 gravitropism (Friml et al., 2002). The gravitropic response mechanism can be divided into  
42 three sequential phases, i) perception of a change in gravity vector, ii) establishment of an  
43 asymmetric auxin distribution and iii) asymmetric growth response (Sato et al., 2015, Singh  
44 et al., 2017). Roots have been suggested to use a tipping point mechanism to reverse the  
45 asymmetric auxin flow at midpoint of bending, allowing to fine tune the root apex position  
46 (Band et al., 2012). During the asymmetry acquisition phase, auxin fluxes are altered  
47 through the differential relocation of auxin efflux transporter PIN-FORMED proteins  
48 (PINs), in particular PIN3 and PIN2, observed 30 min to 2 h after root reorientation (Friml et  
49 al., 2002; Rahman et al., 2010). Gravitropism induces changes in PIN3 polar localization  
50 in root columella where it relocates towards the lower part of the columella cells (Friml et al.,  
51 2002, Grones et al., 2018). Differential regulation of PIN2 trafficking between the upper and  
52 lower surfaces of a gravistimulated root is crucial to maintain modifications of the  
53 concentration of auxin on each side of the root, firstly initiated by PIN3 in the columella cells.  
54 On the lower root side, endocytosis of PIN2 is inhibited, resulting in plasma membrane  
55 maintenance of PIN2 in expanding epidermal cells, while on the upper root side, PIN2 is  
56 rapidly internalized and degraded (Abas et al., 2006). Although PIN1 does not play a direct  
57 role in the differential accumulation of auxin, it is responsible for providing an auxin pathway  
58 to feed the root tip. The asymmetric redistribution of auxin between the lower and upper part  
59 of a gravistimulated root can be revealed by markers like the auxin response reporter DR5  
60 (Ulmasov et al., 1997), the auxin sensor DII (Brunoud et al., 2012) and its ratiometric version  
61 R2D2 (Liao et al., 2015). A decrease in the upper to lower auxin ratio is responsible for the  
62 differential root growth and thus the reorientation of the apex in the downward direction.

63 The *pin2* mutant was firstly described as an agravitropic mutant with a curling of the primary  
64 root, amongst other phenotypes, identified from various genetic screens (Chen et al., 1998;  
65 Luschnig et al., 1998; Müller et al., 1998, Utsuno et al., 1998). This multiple origin is reflected  
66 in its various given names prior to its molecular characterization: *wavy 6 (wav6)*, *ethylene-*  
67 *insensitive root 1 (eir1)*, *agravitropic 1 (agr1)* and finally *pin-formed 2 (pin2)*. An extensive  
68 analysis of the published descriptions of *pin2* root phenotype gives a wide range of  
69 gravitropic responses, from almost entirely gravitropic to a strong loss of gravitropic  
70 response (Fig. 1A). This raises the question of the expressivity of the gravitropic phenotype  
71 in *pin2* and other *pin* mutants. In this study, we identified a new allelic mutant in *PIN2* that we  
72 named *pin2-2* and revealed that *pin2* phenotype is conditional and nutrient-sensitive,  
73 providing an explanation for its phenotypic discrepancy in the scientific literature (Fig. 1B,C).

74 Previous studies have shown that auxin and nutrient transports can compete, resulting in  
75 differential growth or development in various environmental conditions. The nitrate  
76 transporter NRT1.1 has been shown to transport auxin in heterologous systems (Krouk et  
77 al., 2010) providing an elegant explanation of its lateral root growth phenotype. Its role as a  
78 transceptor also suggests pathways for the regulation of PIN proteins. The root coiling on  
79 horizontal growth in nitrate deficiency has been shown to be caused by asymmetric auxin  
80 response (Chai et al., 2020). Presence of nitrate suppresses asymmetric root growth  
81 mediated by the transporter NRT1.1, indeed PIN2-mediated auxin transport is epistatic to  
82 NRT1.1 during nitrate deficiency (Chai et al., 2020). Our study does not suggest similar  
83 competing properties for PIN proteins but demonstrates a differential expression pattern in  
84 various conditions. Indeed, the conditional phenotype of *pin2* is revealed in the presence and  
85 absence of phosphate or nitrate and does not result from osmotic variations. Using slow and  
86 fast auxin reporters, respectively DR5 and R2D2, we showed that auxin asymmetric  
87 accumulation in the root tip is altered by the nutrient's composition of the medium. Further  
88 investigation revealed that ectopic expression of *PIN1* rather than changes in *PIN3* or *AUX1*  
89 is associated with a reversion of the gravitropic phenotype. Taken together, our study  
90 provides insight into the conditional agravitropic phenotype of *pin2* and exposes redundancy  
91 in the PIN family, with an important role for PIN1 in restoration of *pin2* phenotype as an  
92 adaptation to nutrients availability.

93

## 94 2. Materials and Methods

### 95 **2.1. Plant materials, growth conditions, quantification of PR length and growth rate**

96 *Arabidopsis thaliana* Columbia-0 (Col-0) ecotype was used as the wild-type. Mutants and  
97 transgenic lines including *pin2/eir1-1/eir1-4* (Chen et al., 1998; Luschnig et al., 1998), *pin3-5*  
98 (Blilou et al., 2005), *pin1-3* (Bennet et al., 1995), *SALK\_122916* (Alonso et al., 2003) were  
99 described previously. The following transgenic lines were used for expression studies:  
100 DR5:GFP (Benkova et al., 2003), R2D2 (Liao et al., 2015), pPIN3::PIN3-GFP (PIN3:GFP)  
101 (Dello Iorio et al., 2008), pAUX1::AUX1-YFP (AUX1:YFP) (Swarup et al., 2005), pPIN1::PIN1-  
102 GFP (PIN1:GFP) (Omelyanchuk et al., 2016) and were introgressed into the *pin2-2* genetic  
103 background by crossing to generate homozygous lines. For seedlings growing on plates,  
104 *Arabidopsis* seeds were surface-sterilized with a solution containing 12.5: 37.5 : 50 (v/v/v) of  
105 bleach/water/ethanol for 5 min with agitation. Seeds were rinsed three times with 96%  
106 ethanol before drying. Seeds were then germinated on 1/2 Murashige and Skoog basal  
107 medium (MS) supplemented with Gamborg's vitamins (Murashige and Skoog Basal Medium  
108 M0404 - Sigma Aldrich), 0.8% agar, 1% sucrose, 0.05% MES, pH adjusted to 5.7. Plants  
109 were grown under long-day photoperiods (16 h light/8 h dark and a temperature of 21°C with

110 light intensity of  $120 \mu\text{mol cm}^{-2} \text{s}^{-1}$  provided by Osram, Berlin, Germany; 18-W 840 Lumilux  
111 neon tubes). For the experiments carried out on the Root Phenotyping platform using the  
112 The High Resolution Root Scanner (HIRROS) setup (Fernandez et al., 2022) the seedlings  
113 were grown with 1% agar, under long-day photoperiods with LED lighting (between 40 and  
114  $350 \mu\text{mol m}^{-2} \text{s}^{-1}$ ) and a temperature of  $23^{\circ}\text{C}$ .

115 Plants were treated with a supplementation in the medium of 150 mM sorbitol or 75 mM  
116 NaCl or a range (0 g/L, 100g/L, 250 g/L) of PEG-8000 (P2139 - Sigma Aldrich) using a  
117 protocol described previously (Verslues et al., 2006).

118 The different medium compositions are in Materials and Methods Supplemental S1.

119 The primary root (PR) length was quantified using ImageJ software and presented in graphs  
120 with  $n=30$  seedlings. The growth rate was calculated using seedling growth for 24h.

121

## 122 **2.2. Sequencing**

123 Bulk sequencing of *lasso* mutant was done from an F2 after a backcross with Col-0.  
124 Sequencing was produced by BGI with the sequencing platform BGISEQ-500, the read  
125 length used was paired-end 100 bp and the data output was 4G clean data per sample. Low  
126 quality bases were removed using cutadapt, and reads were mapped on Arabidopsis  
127 genome using bwa mem. Then GATK was used to call variants, along with SNPeff to predict  
128 their effect, allowing to quickly find differences between *lasso* and Col-0. All the variations  
129 (SNP or small deletion or insertion) with a potentially large impact on the structure of a gene  
130 was looked.

131

## 132 **2.3. Gravistimulation**

133 Seeds were sowed in sterile condition on MS/2 medium then vernalized for 2 days at  $4^{\circ}\text{C}$  in  
134 the dark. They were placed in culture chamber in vertical position. After 6 days, the  
135 seedlings were transferred to a new plate containing various media or control and rotated  
136  $90^{\circ}$  with respect to the gravitational vector. A quantification of the position of the apex is  
137 carried out at different times and categorized into 8 different orientations on a circular graph  
138 (Swarup et al., 2004 ; Petrášek et al., 2006), detail of the category is in Materials and  
139 Methods Supplemental S2. Adobe Photoshop CS6 was used to overlay gravistimulation  
140 images.

141

## 142 **2.4. Confocal imaging, and fluorescence signal quantification**

143 For fluorescence visualization, Leica SP8 (Leica microsystems, Wetzlar, Germany) coupled  
144 with the LASX software and equipped either with HC PL APO CS2 40x/1.10 water or HC PL

145 APO CS2 63x/1.40 oil was used. Image captures were performed with the same confocal  
146 settings (gain, laser strength, pinhole) to generate comparable images among different  
147 treatments or genetic backgrounds. 6 DAG seedlings were mounted on a slice of medium.  
148 Fluorescence signals for GFP (excitation 488 nm, emission 500 to 540 nm), YFP (excitation  
149 514 nm, 520 to 540 nm) and propidium iodide (excitation 561 nm, emission 580 to 630 nm)  
150 were detected. For image quantification (R2D2, PIN3:GFP, AUX1:YFP, PIN1:GFP,  
151 fluorescence intensity measurements), maximum intensity projections of confocal pictures  
152 were used. Roots were observed respectively 30 min, 1h or 1h30 after gravistimulation for  
153 PIN3:GFP, PIN1:GFP, AUX1:YFP and R2D2. The image analyzes and quantification were  
154 performed using Fiji-ImageJ. The quantification of GFP intensity for DR5:GFP was  
155 performed with the Plot Profile. The intensity of the signal was normalized with area when it  
156 was different and represented as mean signal intensity in arbitrary units (a.u). For R2D2 ,  
157 nuclear signal was quantified in the first 9 cells of epidermis layer as previously described  
158 (Liao et al., 2015). Minimum 10 to 16 independent biological replicates were performed. For  
159 PIN3:GFP, the quantification was done as previously described (Grones et al., 2018). For  
160 AUX1:YFP, the quantification was done along a line passing through the lower and upper  
161 face of the root in response to 1h30 of gravitropism. For PIN1:GFP at first the quantification  
162 was done in a square in the stele after 1h of gravitropism and then in the total epidermis or  
163 directly at the plasma membrane.

164

## 165 **2.5. Statistical analysis**

166 The number of independent repetitions of experiments, as well as exact sample sizes, is  
167 described in the figure legends. Statistical analysis (Student's t-test) were performed using  
168 the software R. Statistical significance was tested as described in the figure legends.

169

## 170 **3. Results**

### 171 **3.1. Identification of the *lasso* (*pin2-2*) mutant**

172 A mutant was identified by screening an activation tagging population (Weigel et al., 2000)  
173 looking for plants with a skewed root in response to salt stress. This mutant displayed a  
174 curled primary root in half MS medium (MS/2) and in presence of NaCl (Fig. S1A). It was  
175 named *lasso* to describe the coiling of its root like a rope (Fig. 2A). Further gravistimulation  
176 experiments were performed on regular half MS medium supplemented with NaCl or sorbitol  
177 to understand how root coiling was impacted. Wild-type Col-0 plants displayed a fully  
178 functional response to gravity in all conditions whereas the *lasso* mutant root was  
179 agravitropic on MS/2 medium, supplemented or not with NaCl. Intriguingly, gravity response  
180 of the mutant was partially restored when grown on MS/2 supplemented with sorbitol (Fig.  
181 S1B). No activation tagging T-DNA was found to co-segregate with the *lasso* phenotype.

182 Instead, bulk sequencing of F2 *lasso* mutants from a wild-type backcross identified a  
183 deletion/insertion event in *PIN2* (AT5G57090). A 30bp deletion from C<sub>638</sub> to A<sub>668</sub> is replaced  
184 by a 19bp insertion (TAACTCCTCCATGATAACG) creating a stop codon in the third exon  
185 (Fig. S1C). Introgression of the *proPIN2:PIN2-GFP* construct into the *pin2-2* genetic  
186 background fully reverted the agravitropic root phenotype, further confirming the  
187 identification of the causal mutation (Fig. S1D). The *lasso* mutant was subsequently  
188 renamed *pin2-2* and was shown to also display a 30% reduction in primary root length (Fig.  
189 S2A) like previously described *pin2* alleles. Similarly to known *pin2* alleles (Ottenschlager et  
190 al., 2003), an accumulation of the auxin reporter DR5-GFP was observed in the root tip  
191 (columella and lateral root cap) of the *pin2-2* mutant (Fig. 2B). Upon gravistimulation, a lack  
192 of asymmetry in auxin distribution was observed in the *pin2-2* background, compared to wild-  
193 type where auxin signal asymmetry is measurable in the lateral root cap (Fig. 2C).

194

### 195 **3.2. *pin2* agravitropic root phenotype is conditional and nutrient-sensitive**

196 Since *pin2-2* displays sensitivity to the composition of the medium, we tested whether  
197 osmolarity impacts root gravity response in *pin2-2*. Polyethylene glycol (PEG), a non-  
198 metabolized polymer, was used to alter osmolarity in the medium. It was previously  
199 demonstrated that root growth is increased at 100 g/L of PEG and inhibited at 250 g/L of  
200 PEG (Rosales et al., 2019). We therefore used both concentrations to dissociate root growth  
201 effects from osmolarity. Position of the root apex was monitored 48h after a 90° reorientation  
202 of the vertical plates and grouped into 8 angular sections (Swarup et al., 2004). Wild-type  
203 seedlings displayed a normal response to gravity in all conditions tested and the *pin2-2*  
204 mutant displayed a strong agravitropic phenotype in all conditions tested (Fig. S1E).  
205 Increasing osmotic pressure did not revert the agravitropic phenotype of *pin2-2* mutant  
206 suggesting that osmolarity alone does not represent a permissive condition.

207

208 In order to determine which nutrient alters *pin2-2* phenotype, we tested the impact of  
209 deficiency in three major nutrients, nitrogen (MS/2-N), phosphorus (MS/2-P) and iron (MS/2-  
210 Fe). A global dilution of the culture medium was also tested by comparing half MS (MS/2) to  
211 one-tenth MS (MS/10). In all conditions tested, wild-type (Col-0) plants responded to gravity  
212 (Fig. 2D). The *pin2-2* mutant showed an agravitropic root growth on MS/2 and MS/2-Fe  
213 medium, thus defining restrictive conditions. However, when grown on MS/2-P, MS/2-N and  
214 MS/10 media the *pin2-2* mutant partially reverted to a wild-type gravitropic response,  
215 defining permissive conditions. It is worth noting that although the phenotype difference is  
216 unambiguous between the 2 conditions, the response to gravity in permissive conditions is  
217 not exactly as total as wild-type. Indeed, the root apex is orientated mostly in sector 6 for  
218 *pin2-2* compared to sectors 5 and 6 for wild-type (Fig. 2D). Also, the primary root of the *pin2-*

219 *pin2* mutant shows a slight curvature whereas that of the wild-type plants is perfectly straight  
220 (Fig. 2D). This conditional phenotype was tested on the available allelic series of *pin2*  
221 mutants: *eir1-1*, *eir1-4* and a T-DNA mutant from SALK (*SALK\_122916*). All *pin2* alleles  
222 tested showed a conditional agravitropic root phenotype with identical permissive and  
223 restrictive conditions (Fig. S2B,C). These results confirm that the *pin2* mutant agravitropic  
224 root phenotype is conditional and nutrient-sensitive.

225

### 226 **3.3. Conditional *pin2* phenotype does not result from defects in growth or early** 227 **gravitropism and is not observed in *pin1* and *pin3***

228

229 We tested whether mutants in the main PIN transporters expressed in the root tip could  
230 share a similar conditional root gravitropic phenotype as *pin2* (Table 1). PIN1 controls the  
231 main auxin flow to the root tip and PIN3 has been shown to relocalize auxin upon  
232 gravistimulation in the columella cells (Omelyanchuk et al., 2016; Friml et al., 2002). In both  
233 permissive and restrictive conditions, we observed a wild-type gravitropic response of *pin1*  
234 and *pin3*, 48 hours after induction (Fig. S3). We next tested the very early gravitropic  
235 response (up to 9 hours) and whether growth defects could be linked with the conditional  
236 phenotype of *pin2*. The kinetics of root curvature were monitored 0, 3, 6 and 9 h after  
237 gravistimulation (Fig. S4). All mutants tested (*pin1*, *pin2* and *pin3*) showed a root bending  
238 response similar to wild-type (Table 1) demonstrating that the early gravitropic response was  
239 not altered in any of the 3 *pin* mutants. Growth rate was evaluated over 24 hours post-  
240 gravitropic induction and showed a global reduction of root growth for all *pin* mutants tested  
241 (Fig. S5). However, no correlation with permissive and restrictive conditions were observed,  
242 suggesting that root growth alteration is not responsible for the phenotypic expression and  
243 reversion of *pin2* (Table 1). These results suggest that *pin2*, but not *pin1* or *pin3*, display a  
244 conditional agravitropic root phenotype that does not involve early gravitropic response or  
245 root growth defects.

246

### 247 **3.4. Auxin accumulation is modulated by nutrient availability**

248

249 The late auxin response marker DR5 fused to GFP (Ulmasov et al., 1997) was used to  
250 monitor auxin accumulation in the root tip 4 hours after plant gravistimulation. Permissive  
251 conditions (MS/10, MS/2-P and MS/2-N) had no effect on the wild-type auxin profile but  
252 resulted in a global reduction of the intensity of DR5-GFP both in the central zone and in the  
253 lateral root cap of *pin2* compared to restrictive conditions (MS/2 and MS/2-Fe) (Fig. S6).  
254 However, no asymmetric accumulation could be revealed using this marker in the mutant  
255 plant whereas it was observed in the wild-type plants in both conditions, suggesting either



256 that auxin asymmetry is not restored in the *pin2-2* mutant in permissive conditions or that  
257 DR5 is not a dynamic enough marker to monitor such changes.  
258 We therefore used the ratiometric version of the DII marker (R2D2) to observe dynamic  
259 changes in auxin response as the degron (DII) motif of Aux/IAA is degraded upon auxin  
260 application within minutes (Liao et al., 2015). We were able to monitor auxin changes 90  
261 minutes after plant gravistimulation (Fig. 3A,S7A). Data are presented as the mDII/DII  
262 (modified non-degraded DII to DII) ratio therefore showing an increase in ratio when more  
263 auxin response is occurring and DII is degraded (Fig. 3B,C). Wild-type (Col-0) plants  
264 displayed an increased auxin response on the lower epidermal layer (first nine epidermal  
265 cells) compared to the upper side (Fig. 3B,C). Some medium compositions slightly altered  
266 the auxin response levels in the wild-type plants. Indeed, conditions MS/2-Fe globally  
267 reduced both upper and lower auxin response whereas conditions MS/2-N and MS/10  
268 reduced only auxin response in the lower side. These reductions were not associated with  
269 any root gravitropic defects. In the *pin2-2* mutant background, auxin signals were also  
270 reduced depending on the conditions. Only permissive conditions were associated with a  
271 reduction on the auxin response both in the upper and lower epidermal cell files (first nine  
272 epidermal cells). In this case, reduction of the mDII/DII ratio was associated with the  
273 phenotypic reversion of the root gravitropic response in *pin2-2*. However, this change in  
274 auxin response was not associated with a strong reduction of the up to down ratio  
275 demonstrating that auxin levels in the *pin2-2* mutant remain high compared to wild-type  
276 plants (Fig. S7B). Altogether, these results suggest that a reduction of the auxin signal in the  
277 *pin2-2* elevated auxin background would be responsible for the phenotypic reversion.

278

### 279 **3.5. PIN3 and AUX1 protein accumulation is not altered in *pin2***

280 In order to identify a molecular mechanism responsible for the changes in auxin response in  
281 various nutrient conditions, we monitored the expression of the PIN3 and AUX1 proteins, two  
282 key players of the root gravitropic response in plants (Friml et al., 2002; Groner et al., 2018).  
283 The PIN3:GFP reporter line was used to monitor PIN3, which is localized to the plasma  
284 membrane in the columella and known for its rapid relocation following gravistimulation. In  
285 both the wild-type (Col-0) and *pin2-2* backgrounds, observation of PIN3-GFP after 30  
286 minutes of gravistimulation (Fig. 4A,S8) showed a greater accumulation on the lower side  
287 independently of the medium composition used (Fig. 4B). We next used the AUX1:YFP  
288 reporter line to monitor AUX1 accumulation, an auxin influx transporter localized in the  
289 lateral root cap and epidermis whose expression mediates auxin transport from the root cap  
290 towards the epidermal cells during the gravitropic response (Bennet et al., 1996 ; Swarup et  
291 al., 2001). Observation of AUX1-YFP in both the wild-type (Col-0) and *pin2-2* backgrounds  
292 after 1h30 of gravistimulation (Fig. 4C,S9A) showed no changes in localization pattern. The

293 measure up to down ratio was close to 1, suggesting the absence of asymmetric distribution  
294 of AUX1 (Fig. 4D). Medium composition still had an impact on AUX1:YFP intensity without  
295 affecting this ratio (Fig. S9B). These results show that the symmetry of AUX1 and PIN3  
296 protein accumulation profiles is not affected by either the *pin2-2* mutation or changes in  
297 medium composition, and likely do not play a role in the conditional reversion of the *pin2*  
298 phenotype.

299

### 300 **3.6. Ectopic expression of PIN1 in the epidermis is associated with the phenotypic** 301 **reversion of *pin2***

302 We next monitored the localisation of PIN1 using the PIN1-GFP reporter line (Huang et al.,  
303 2010). The auxin efflux transporter is present in the basal plasma membrane in the stele  
304 cells where it directs auxin transport to the apex (Omelyanchuk et al., 2016). Expression of  
305 PIN1-GFP was observed 1 hour after gravistimulation. A decrease in the presence of PIN1  
306 in the stele was observed on MS/2-Fe, MS/2-P, MS/2-N, MS/10 in wild-type plants (Fig.  
307 S10A,B). There was a reduction in PIN1 accumulation in the stele in *pin2-2* compared to  
308 Col-0 but because auxin levels remain high in the *pin2-2* columella (Fig. 2B), this suggests  
309 that this reduction has no impact on auxin accumulation in the tip.

310 Previous reports have shown that ectopic expression of PIN1 can be seen in the epidermal  
311 cells in the *pin2* mutant background (Vieten et al., 2005). We therefore monitored PIN1  
312 protein localization in the epidermis and found that there is no accumulation in wild-type  
313 plants in this tissue that could be detected by laser scanning confocal microscopy (Fig.  
314 5A,S10C). Quantification therefore provided a background noise level to which other  
315 conditions were compared (Fig. 5B,C). In the *pin2-2* mutant background, in all condition  
316 tested, the signal of epidermal PIN1-GFP was systematically detected (Fig. 5B) and the  
317 number of cells with a positive GFP signal was between 30 and 40 compared to less than 10  
318 in wild-type (equivalent to noise level – Fig. 5C). Using higher magnification, we were able to  
319 confirm PIN1-GFP signal at the membrane of epidermal cells in the *pin2-2* mutant only (Fig.  
320 5D). Quantification of this signal revealed that PIN1-GFP is expressed almost symmetrically  
321 in restrictive conditions (MS/2 and MS/2-Fe) with a ratio of 1 to 1.5 and a strong asymmetry  
322 is established in permissive conditions (MS/2-P, MS/2-N and MS/10) with a ratio value  
323 ranging from 3 to 5 (Fig. 5E). These observations demonstrate that nutrient composition can  
324 alter PIN1 protein accumulation in the *pin2* mutant background, associated with a restoration  
325 of the root gravitropic response.

326

## 327 4. Discussion

### 328 **4.1. PIN proteins play a complex and redundant role in physiology and development**

329 Despite being a well-characterized family of proteins, PINs still keep secrets regarding their  
330 mode of action. Recently, the structures and mechanisms of PIN1, PIN3 and PIN8 were  
331 reported (Yang et al., 2022; Su et al., 2022, Ung et al., 2022) but how their biochemical  
332 activity is further integrated in a complex multicellular organism, largely controlled by direct  
333 environmental interactions remains poorly understood. The early identification of *pin* mutants  
334 led to the description of major developmental events controlled by this redundant family of  
335 genes and to a better understanding of the underlying role of the major phytohormone auxin  
336 (reviewed by Krecek et al, 2009; Sauer and Kleine-Vehn, 2019). Surprisingly, the *pin2*  
337 mutant phenotype has suffered a lack of detailed description at the root level and has  
338 certainly come across as a weak gravitropic mutant due to the heterogeneity of  
339 observations, as reflected in the literature and summarized in Figure 1.

340

#### 341 **4.2. The *pin2* mutant lacks the ability to establish asymmetric auxin response...**

342 Here, we report that *pin2* root agravitropic phenotype is conditional and nutrient-sensitive,  
343 providing an explanation for previous observations. Our study pinpoints that the wide  
344 heterogeneity of growth conditions used in the many laboratories involved (nutrients but also  
345 light intensity, temperature, photoperiod etc...) strongly affects conclusions about the role of  
346 given protein/gene families. In the case of *pin2*, we demonstrate that early response to  
347 gravity is intact (Table 1). However, *pin2* roots coil like a lasso in restrictive conditions after  
348 this brief period of gravitropic primary root growth (Fig. 1B,2A). The intensive coiling of this  
349 mutant suggests a loss of the ability to establish asymmetric auxin flows and probably also  
350 to return to a symmetric repartition. Indeed, it is well known that *pin2* accumulates auxin at  
351 the root tip (Ottenschläger et al., 2003) due to the lack of transport back towards the  
352 epidermis, where it is normally expressed (Blilou et al., 2005). This overaccumulation of  
353 auxin triggers events that are unique amongst other agravitropic mutants such as *aux1*.  
354 Indeed, the *aux1* mutant root is agravitropic from germination onward. This is due to the lack  
355 of auxin transport from the lateral root cap towards the epidermis (Swarup et al., 2005),  
356 however no overaccumulation of auxin is present in the root tip suggesting that the rapidity  
357 of auxin redistribution rather than its actual long-term transport is responsible for the  
358 agravitropic phenotype. In the present study, we found that AUX1 protein accumulation  
359 profile was not altered in the *pin2* mutant background suggesting that this protein does not  
360 contribute to the conditionality of the phenotype. The high levels of auxin in the *pin2* mutant  
361 apex most likely prevent the action of other PIN transporters (such as PIN3) to promote  
362 asymmetric redistribution of auxin. In the first few days of *pin2* mutant growth, plants still  
363 manage to grow along the gravity vector, probably due to the time it takes to build up the  
364 auxin accumulation in the apex. Then the primary root starts to coil continuously.

365

#### 366 **4.3. ...but nutrients can revert *pin2* phenotype by modulating auxin fluxes**

367 The reversibility of *pin2* root phenotype suggests that environmental conditions can modify  
368 auxin fluxes within the plant. It has been reported previously that nutrients can alter the  
369 gravitropic response of plants. Indeed, studies on the effect of nitrate on primary root coiling  
370 have shown that *pin2* mutants are less sensitive to nitrate-induced coiling (Chai et al., 2020).  
371 Since these experiments were performed on horizontal plates, they encompass both  
372 gravitropic and thigmotropic responses, and their effect in the longer term. This study  
373 nevertheless suggests a link between gravitropism and nutrient availability.

374 This result is reminiscent of the ability of the nitrate transporter NRT1.1 to transport auxin  
375 competitively, providing an explanation for the lateral root growth phenotype of the  
376 *chl1/nrt1.1* mutant (Krouk et al., 2010). Here, we observed the ectopic expression of PIN1 in  
377 the epidermal cells in the *pin2* mutant background as reported previously (Vieten et al.,  
378 2005) and seen in the wild-type background upon application of aluminium or flavonols (Li et  
379 al., 2021; Santelia et al. al., 2008). Interestingly, the asymmetric distribution of PIN1 in this  
380 tissue remains at a ratio value close to 1-1.5 in restrictive conditions. However, in permissive  
381 conditions, this up-to-down ratio is higher (3 to 5) suggesting that the subsequent restoration  
382 of asymmetric auxin fluxes would be responsible for the phenotypic change. Although PIN1  
383 accumulation in the apical membrane of the epidermal cells is always at least slightly  
384 asymmetric, we suggest the existence of a threshold value below which no phenotypic  
385 restoration occurs (in restrictive conditions) and above which agravitropic restoration  
386 happens (in permissive conditions). This ratio threshold is situated between 2 and 3.  
387 Subsequent studies should further define how changes in nutrient composition can modulate  
388 PIN1 expression in a direct or indirect manner. In this study, we limited the analysis to major  
389 nutrients such as nitrate, phosphate and iron because they are major elements regulating  
390 root growth and development (Xuan et al., 2017; Liu 2021; Liang 2022). We defined  
391 permissive conditions based on a widely used medium, which is the half-diluted Murashige  
392 and Skoog medium but virtually infinite modulations of medium composition could be tested.  
393 Since both nitrate and phosphate starvations, as well as one tenth diluted MS, define  
394 permissive conditions, we did not investigate the downstream pathways of particular  
395 elements. Numerous regulators have been identified as regulators of starvation response to  
396 nitrate (Kiba et al., 2018) and phosphate (Rouached et al., 2010) and even common  
397 elements are known (Ristova and Kopriva, 2022). However, no molecular link has been  
398 shown between these pathways and PIN1 expression in the root epidermis. Further studies  
399 should provide more information towards this goal. These would help understand how  
400 gravitropism is modulated by nutrients in the *pin2* mutant.

401 Indeed, our observations show that the phenotypic change only occurs in the mutant  
402 background, pinpointing the need for the ectopic expression of PIN1 in this context for a

403 plant root facing an heterogeneous soil. This observation fits with known characteristics of  
404 the PIN gene family. Indeed, PIN genes are known to show strong redundancy and changes  
405 in expression based on auxin induction (Vieten et al., 2005). Moreover, our results show that  
406 in the wild-type plants, nutrients have a measurable impact on auxin response (using R2D2  
407 reporter) that could be the basis for a fine modulation of root gravitropism in soil where  
408 numerous factors can be altered simultaneously (nutrients, physical contact, water...). These  
409 observations suggest that the relation between root tropisms and nutrients, but also water  
410 and physical stress should be further investigated.

411

## 412 5. Conclusion

413

414 In this study, we provide evidence for a conditional phenotype of the *pin2* mutant and a link  
415 between nutrients and auxin transport/response (Fig. 6). Modulation of auxin transport  
416 through differential PIN expression in various environmental conditions alters root gravitropic  
417 response and suggests that this tropic response has been under strong selective pressure to  
418 promote a fine-tuning of soil exploration. Interestingly, the rice mutant in *PIN2*, *Ospin2*, as  
419 well as that of *AUX1*, *Osaux1* are not totally agravitropic, but instead display a root growth  
420 angle defect (Inahashia et al., 2018, Giri et al., 2018). This suggests that defining root growth  
421 angle by modulating the gravitropic response can be controlled both genetically and  
422 environmentally. These observations open the way to improving root exploration in crops for  
423 a better use of resources.

424

## 425 Funding

426 This research was supported by Institut Agro Montpellier and the GAIA doctoral school via a  
427 doctoral grant.

428

## 429 Credit authorship contribution statement

430 BP, FD, and MaT contributed to conception and design of the study. MaT, FD, CO  
431 performed the acquisition, analysis and interpretation of data. AC and PN were in charge of  
432 creating and maintaining the phenotyping platform for dynamic root growth analysis. AS and  
433 FD analyzed the sequencing of the *lasso* mutant. MeT and EH contributed to the initial  
434 forward genetics screen to discover the new *lasso* mutant. BP and MaT wrote the article.

435

## 436 Acknowledgments

437 We also acknowledge Prof. Hidehiro Fukaki (Kobe University, Japan) and Tatsuaki Goh  
438 (Nara, Japan) for sharing their *eir1-1* and *eir1-4* seeds. We acknowledge the imaging facility  
439 MRI, member of the France-Biolmaging infrastructure supported by the French National

440 Research Agency (ANR-10-INBS-04, “Investments for the future”) and especially Dr Carine  
441 Alcon for her valuable comments and technical assistance on microscopy imaging.

442

443 Declaration of Competing Interest

444 The authors declare that they have no competing financial interests or personal relationships  
445 that could have appeared to influence the work reported in this paper.

446

447 Figure captions

448

449 **Figure 1. Literature description of the agravitropic root phenotype of *pin2* is**  
450 **heterogeneous**

451 **(A)** Representative drawing of *pin2* mutant’s phenotype drawn from previous reports **1.** Allele  
452 *Atpin2::En701* grown on Murashige and Skoog (MS) medium (Müller *et al.*, 1998) **2.** Allele *eir1-3*  
453 grown on unsupplemented plant nutrient agar (PNA) without sucrose (Luschnig *et al.*, 1998) **3.** Allele  
454 not specified grown on MS medium (Blakeslee, *et al.*, 2007) **4.** Allele *eir1-4* grown on MS/2 medium or  
455 PNS (Retzer *et al.*, 2017) **5.** Allele N591142 (*pin2-T*) grown on MS medium (Liu *et al.*, 2018) **6-.** Allele  
456 *eir1-4* grown on PNS (Retzer *et al.*, 2019) **7.** Allele *eir1-4* grown on Hoagland medium (Ashraf *et al.*,  
457 2020) **8.** Allele not specified grown on MS/2 medium (Wu *et al.*, 2021) **(B)** Representative drawing of  
458 *pin2-2* mutant phenotype used in the present study **1.** Plants grown in repressive conditions (MS/10).  
459 **2.** Plants grown in permissive conditions (MS/2) **(C)** Representative picture of *pin2-2* in repressive  
460 (MS/10) or repressive (MS/2) conditions, stars indicate plants selected for drawing.

461

462

463 **Figure 2. The agravitropic root growth phenotype of *pin2-2* is conditional and nutrient-**  
464 **sensitive**

465 **(A)** Agravitropic root phenotype of the *pin2-2* mutant allele (11-day-old seedlings grown on MS/2  
466 medium). Inlay: zoom in on the “lasso” root coil. Black scale bar = 1 cm, white scale bars = 1mm. **(B)**  
467 Representative confocal images of the root apex stained with propidium iodide (cyan) of DR5-GFP  
468 expressing plants (fuchsia). White arrows indicate auxin accumulation in the lateral root cap. Dotted  
469 white lines indicate the position where GFP intensity was measured. Seedlings were grown vertically  
470 for 6 days and then transferred horizontally for 4 h on an MS/2 medium. g: gravity vector, scale bar =  
471 50 microns. **(C)** DR5-GFP intensity was quantified with the Plot ImageJ profile and displayed along  
472 the position of the root,  $16 < n < 20$  **(D)** Gravitropic response of wild-type (Col-0) and *pin2-2* mutants. 6-  
473 day-old seedlings were grown on vertical plates then rotated 90° and imaged after 48 hours. Circular  
474 diagrams display the primary root apex orientation as colored bars representing the percentage of  
475 plants. n=30, scale bar = 1cm.

476

477 **Table 1. Gravitropic response and growth rate of *pin1*, *pin2* and *pin3* in permissive**  
478 **and restrictive conditions**

479 Summarized table of *pin1*, *pin2-2* and *pin3* early and late gravitropic response and root growth. Early  
480 gravitropism: 6-day-old seedlings were subjected to a 90° gravitropic stimulus and imaged at 3, 6 and  
481 9 hours. Representative image of data presented in Figure S4. Gravitropism: 6-day-old seedlings  
482 were subjected to a 90° gravitropic stimulus and imaged after 48h. Representative image of data  
483 presented in Figure S3. Growth: primary root growth of 6-day-old seedlings was monitored for 24  
484 hours (n=20) and expressed as the average +/- standard error in mm per day. Representative graph  
485 of data presented in Figure S5. Green ticks indicate gravity response while a red cross indicates an  
486 agravitropic response. Scale bar = 1cm.

487

### 488 **Figure 3. Auxin accumulation is modulated by nutrient availability**

489 **(A)** Representative confocal image of the ratiometric sensor R2D2 showing DII-n3xVenus (green) and  
490 mDII-ndtTomato (purple) signals. White areas represent the first 9 epidermal cells chosen for  
491 quantification. 6-day-old seedlings were imaged on a microscopy slide with a block of MS/2 medium  
492 1h30 after gravistimulation. g = gravity vector, scale bar = 50 microns **(B,C)** Quantification of the  
493 mDII/DII ratio in the first 9 epidermal cells in the up or down part of the root tip 1h30 after  
494 gravistimulus in wild-type (Col-0) and *pin2-2* in various media (MS/2, MS/10, MS/2-P, MS/2-N, MS/2-  
495 Fe). The p-values are based on Student's t-tests for a pairwise comparison relative to reference  
496 medium (MS/2) p<0.0001 (\*\*\*), p<0.001 (\*\*), and p<0.05 (\*), n=15, error bars represent standard  
497 deviation.

498

### 499 **Figure 4. Localization of PIN3 and AUX1 proteins is not altered in the *pin2* mutant** 500 **background in various growth medium**

501 **(A)** Representative confocal image of PIN3:GFP. 6-day-old seedlings were transferred on a horizontal  
502 microscopy slide with a block of MS/2 medium and imaged 30 min after gravistimulation. White lines  
503 represent the position where GFP intensity was measured. g = gravity vector, scale bar = 50 microns  
504 **(B)** Graph representing PIN3:GFP average lower outer/upper outer signal ratio after 30min of  
505 gravitropism of Col-0 and *pin2-2* in response to different media (MS/2, MS/10, MS/2-P, MS/2-N, MS/2-  
506 Fe). The p-values are based on Student's t-tests and the comparison is made for each genotype in  
507 MS/2 compared to the different media tested P <0.0001 (\*\*\*), P <0.001 (\*\*), and P <0.05 (\*), n=15,  
508 error bars represent standard deviation **(C)** Representative confocal image of AUX1:YFP. 6-day-old  
509 seedlings were transferred on a horizontal microscopy slide with a block of MS/2 medium and imaged  
510 90 min after gravistimulation. g = gravity vector, scale bar = 50 micron **(D)** Graph representing the  
511 intensity of AUX1:YFP on the lower and upper face of the root in response to 1h30 of gravitropism of  
512 Col-0 and *pin2-2* in response to different media (MS/2, MS/10, MS/2-P, MS/2-N, MS/2-Fe). The p-  
513 values are based on Student's t-tests and the comparison is made for each genotype in MS/2  
514 compared to the different media tested p<0.0001 (\*\*\*), p<0.001 (\*\*), and p<0.05 (\*), n=15, error bars  
515 represent standard deviation.

516

### 517 **Figure 5. PIN1 is present in the epidermis in the *pin2* mutant background and is** 518 **modulated by nutrient availability**

519 **(A)** Representative confocal image of PIN1:GFP in Col-0 and *pin2-2*. 6-day-old seedlings were  
520 transferred on a horizontal microscopy slide with a block of MS/2 medium and imaged 1h after  
521 gravistimulation. White squares represent the position where GFP intensity was measured. g = gravity  
522 vector, scale bar = 50 micron. **(B)** Graph representing the mean of intensity of PIN1:GFP up + down in  
523 response to 1h of gravitropism in Col-0 and *pin2-2* in response to different media (MS/2, MS/10,  
524 MS/2-P, MS/2-N, MS/2-Fe). The p-values are based on Student's t-tests and the comparison is made  
525 for each genotype in MS/2 compared to the different media tested P <0.001 (b), and P <0.05 (a),  
526 n=15, error bars represent standard deviation. **(C)** Graph representing the epidermal cell count with  
527 PIN1:GFP signal (up+down) in response to 1h of gravitropism in Col-0 and *pin2-2* in response to  
528 different media. The p-values are based on Student's t-tests and the comparison is made for each  
529 genotype in MS/2 compared to the different media tested P <0.0001 (c), P <0.001 (b), and P <0.05  
530 (a), n=15, error bars represent standard deviation. **(D)** Representative confocal image of PIN1:GFP in  
531 Col-0 and *pin2-2*. 6-day-old seedlings were transferred on a horizontal microscopy slide with a block  
532 of MS/2 medium and imaged 1h after gravistimulation. White squares represent a zoom of up and  
533 down epidermis. g = gravity vector, scale bar = 20 micron and scale bar in the zoom = 5 micron. **(E)**  
534 Graph representing the ratio down/up of the intensity of PIN1:GFP at the plasma membrane in  
535 response to 1h of gravitropism in Col-0 and *pin2-2* in response to different media. The p-values are  
536 based on Student's t-tests and the comparison is made for each genotype in MS/2 compared to the  
537 different media tested P <0.0001 (\*\*\*), P <0.001 (\*\*), and P <0.05 (\*), 10<n<16  
538

### 539 **Figure 6. A model for *pin2* conditional agravitropic root phenotype**

540 Proposed model explaining how epidermal ectopic expression of *PIN1* in the *pin2* mutant in  
541 permissive conditions re-establishes asymmetrical auxin fluxes. In the wild-type (Col-0) background,  
542 *PIN2* protein localization in the epidermis drives auxin fluxes and promotes asymmetrical distribution  
543 after a gravistimulus in all conditions tested in this study (restrictive and permissive conditions). In the  
544 *pin2* mutants, *PIN1* ectopic expression in the epidermis is observed in all conditions tested. In  
545 permissive conditions, *PIN1* up-to-down ratio reaches a threshold value and restores an asymmetric  
546 auxin flux that is responsible for the gravitropic response. This mechanism is absent in restrictive  
547 conditions where *pin2* root still grows agravitropically and forms a lasso shape.  
548

### 549 **Figure S1. A new allele of *pin2* mutant discovered in a forward genetics screen**

550 **(A)** Representative picture of the new mutant *lasso* on a forward genetics screening on MS/2  
551 and MS/2 supplemented with 75 mM of NaCl. **(B)** Representative picture of Col-0 and *lasso*  
552 on MS/2 and MS/2 supplemented with 75 mM of NaCl or 150 mM of Sorbitol. 6-day-old  
553 seedlings were transferred on medium and subjected to a 90° gravitropic stimulus and  
554 imaged after 48h in the phenotyping robot HIRROS. **(C)** Representation of the *PIN2* gene  
555 with alignment of reads for Col-0 and *lasso*. The inlay represents a zoom of the *pin2-2*  
556 mutation area noted with the red star on the gene. **(D)** Representative picture of 7-day-old  
557 seedlings of Col-0 and *pin2-2* and the introgression of *proPIN2:PIN2-GFP* construct into



558 *pin2-2* genetic background. scale bar = 1cm (E) Osmotic stress mimicked with the presence  
559 of a range of PEG for Col-0 and *pin2-2*. 6-day-old seedlings were transferred on medium  
560 and subjected to a 90° gravitropic stimulus and imaged after 48h. Circular diagrams display  
561 the primary root apex orientation as colored bars representing the percentage of plants.  
562 n=15, scale bar = 1cm

563

#### 564 **Figure S2. Several *pin2* allelic mutants have a conditional agravitropic phenotype**

565 (A) Graph representing length of Col-0 and *pin2-2* primary root in MS/2. The p-values are based on  
566 Student's t-tests and the comparison is made between Col-0 and *pin2-2* P<0.0001 (\*\*\*), P <0.001 (\*\*),  
567 and P <0.05 (\*), n=15, error bars represent standard deviation. (B) Representative picture of 10-day-  
568 old seedlings of Col-0, *pin2-2*, *eir1-1*, *eir1-4* and *SALK\_122916* mutants on MS/2. Inlay: zoom in on  
569 the root coil. (C) Gravitropic response *eir1-1*, *eir1-4* and *SALK\_122916* mutants. 6-day-old seedlings  
570 were grown on vertical plates then rotated 90° and imaged after 48 hours. Circular diagrams display  
571 the primary root apex orientation as colored bars representing the percentage of plants. n=15, scale  
572 bar = 1cm.

573

#### 574 **Figure S3. Gravitropism response of *pin1*, *pin2* and *pin3* in permissive and restrictive** 575 **conditions**

576 Representative image of 6-day-old seedlings of Col-0, *pin1*, *pin2-2* and *pin3* mutants subjected to a  
577 90° gravitropic stimulus and imaged after 48h in response to different nutrient deficient media (MS/2,  
578 MS/2-Fe, MS/2-P, MS/2-N, MS/10). Circular diagrams display the primary root apex orientation as  
579 colored bars representing the percentage of plants. 15<n<30, scale bar = 1cm.

580

#### 581 **Figure S4. Early gravitropism of *pin1*, *pin2* and *pin3* in permissive and restrictive** 582 **conditions**

583 Representative image of 6 day-old seedlings of Col-0, *pin1*, *pin2-2* and *pin3* mutants subjected to a  
584 90° gravitropic stimulus and imaged at 3, 6 and 9 hours in response to different nutrient deficient  
585 media (MS/2, MS/2-Fe, MS/2-P, MS/2-N, MS/10).

586

#### 587 **Figure S5. Growth rate of *pin1*, *pin2* and *pin3* in permissive and restrictive conditions**

588 Graph representing the primary root growth of 6 day-old seedlings of Col-0, *pin1*, *pin2-2* and *pin3*  
589 mutants monitored for 24 hours (15<n<30) in response to different media (MS/2, MS/10, MS/2-P,  
590 MS/2-N, MS/2-Fe). The p-values are based on Student's t-tests and the comparison is made for each  
591 genotype in MS/2 compared to the different media tested P <0.0001 (\*\*\*), P <0.001 (\*\*), and P <0.05  
592 (\*), error bars represent standard deviation

593

#### 594 **Figure S6. Auxin accumulation is modulated by nutrient availability**

595 Seedlings of Col-0 and *pin2-2* were grown for 6 days vertically and then transferred horizontally for 4  
596 h on the different medium. DR5-GFP intensity was quantified with the Plot ImageJ profile and  
597 displayed along the position of the root, 16<n<20

598

### 599 **Figure S7. Auxin accumulation is modulated by nutrient availability**

600 **(A)** Representative confocal image of the ratiometric sensor R2D2 showing DII-n3xVenus (green) and  
601 mDII-ndtTomato (purple) signals in Col-0 and *pin2-2* in response to various media (MS/2, MS/10,  
602 MS/2-P, MS/2-N, MS/2-Fe). 6-day-old seedlings were imaged on a microscopy slide with a block of  
603 MS/2 medium 1h30 after gravistimulation. g = gravity vector, scale bar = 50 microns **(B)** Quantification  
604 of the lower/upper ratio of mDII/DII ratio in the first 9 epidermal cells in the up or down part of the root  
605 tip 1h30 after gravistimulus in wild-type (Col-0) and *pin2-2* in various media (MS/2, MS/10, MS/2-P,  
606 MS/2-N, MS/2-Fe). The p-values are based on Student's t-tests for a pairwise comparison relative to  
607 reference medium (MS/2)  $p < 0.0001$  (\*\*\*),  $p < 0.001$  (\*\*), and  $p < 0.05$  (\*),  $n = 15$ , error bars represent  
608 standard deviation.

609

### 610 **Figure S8. Localization of proteins is not altered in the *pin2* mutant background in 611 various growth medium**

612 Representative confocal image of PIN3:GFP in response to various media (MS/2, MS/10, MS/2-P,  
613 MS/2-N, MS/2-Fe). 6-day-old seedlings were transferred on a horizontal microscopy slide with a block  
614 of medium and imaged 30 min after gravistimulation. g = gravity vector, scale bar = 50 micron

615

### 616 **Figure S9. Localization of AUX1 proteins is not altered in the *pin2* mutant background 617 in various growth medium**

618 **(A)** Representative confocal image of AUX1:YFP. 6-day-old seedlings were transferred on a  
619 horizontal microscopy slide with a block of various medium and imaged 90 min after gravistimulation.  
620 g = gravity vector, scale bar = 50 micron. **(B)** Graph representing the intensity of AUX1:YFP on the  
621 lower and upper face of the root in response to 1h30 of gravitropism of Col-0 and *pin2-2* in response  
622 to different media (MS/2, MS/10, MS/2-P, MS/2-N, MS/2-Fe). The p-values are based on Student's t-  
623 tests and the comparison is made for each genotype in MS/2 compared to the different media tested  
624  $p < 0.0001$  (\*\*\*),  $p < 0.001$  (\*\*), and  $p < 0.05$  (\*),  $n = 15$ , error bars represent standard deviation.

625

### 626 **Figure S10. PIN1 is present in the epidermis in the *pin2* mutant background and is 627 modulated by nutrient availability**

628 **(A)** Representative confocal image of PIN1:GFP in Col-0 and *pin2-2*. 6-day-old seedlings were  
629 transferred on a horizontal microscopy slide with a block of MS/2 medium and imaged 1h after  
630 gravistimulation. White squares represent the position where GFP intensity was measured. g = gravity  
631 vector, scale bar = 50 micron. **(B)** Graph representing the mean of intensity of PIN1:GFP in the stele  
632 in response to 1h of gravitropism in Col-0 and *pin2-2* in response to different media (MS/2, MS/10,  
633 MS/2-P, MS/2-N, MS/2-Fe). The p-values are based on Student's t-tests and the comparison is made

634 for each genotype in MS/2 compared to the different media tested  $P < 0.001$  (b), and  $P < 0.05$  (a),  
635  $n=15$ , error bars represent standard deviation. **(C)** Representative confocal image of PIN1:GFP in  
636 Col-0 and *pin2-2* in response to different media (MS/2, MS/10, MS/2-P, MS/2-N, MS/2-Fe). 6-day-old  
637 seedlings were transferred on a horizontal microscopy slide with a block of medium and imaged 1h  
638 after gravistimulation. g = gravity vector, scale bar = 50 micron

639

640

#### 641 **Materials and Methods Supplemental S1. Media composition**

642

#### 643 **Materials and Methods Supplemental S2. Circular diagram used for gravitropic** 644 **phenotyping of the root apex upon gravistimulation.**

645

646

647

648

#### 649 References

650 **Abas L, Benjamins R, Malenica N, Paciorek T, Wi J, Anzola JCM, Sieberer T, Luschnig**

651 **C** (2006) Intracellular trafficking and proteolysis of the Arabidopsis auxin-efflux  
652 facilitator PIN2 are involved in root gravitropism. *Nat. Cell Biol.* 8:

653 **Alonso JM, Stepanova AN, Leisse TJ, Kim CJ, Chen H, Shinn P, Stevenson DK,**  
654 **Zimmerman J, Barajas P, Cheuk R, et al** (2003) Genome-wide insertional  
655 mutagenesis of *Arabidopsis thaliana*. *Science* (80- ) **301**: 653–657

656 **Ashraf MA, Umetsu K, Ponomarenko O, Saito M, Aslam M, Antipova O, Dolgova N,**  
657 **Kiani CD, Nehzati S, Tanoi K, et al** (2020) PIN FORMED 2 Modulates the Transport of  
658 Arsenite in *Arabidopsis thaliana*. *Plant Commun* 1: 100009

659 **Band LR, Wells DM, Larrieu A, Sun J, Middleton AM, French AP, Brunoud G, Sato EM,**  
660 **Wilson MH, Peřet B, et al** (2012) Root gravitropism is regulated by a transient lateral  
661 auxin gradient controlled by a tipping-point mechanism. *Proc Natl Acad Sci U S A* **109**:  
662 4668–4673

663 **Benková E, Michniewicz M, Sauer M, Teichmann T, Seifertová D, Jürgens G, Friml J**  
664 (2003) Local, efflux-dependent a module for plant organ formation. *Cell* **115**: 591–602

665 **Bennett SRM, Alvarez J, Bossinger G, Smyth DR** (1995) Morphogenesis in pinoid  
666 mutants of *Arabidopsis thaliana*. *Plant J* **8**: 505–520

667 **Blakeslee JJ, Bandyopadhyay A, Ok RL, Mravec J, Titapiwatanakun B, Sauer M,**  
668 **Makam SN, Cheng Y, Bouchard R, Adamec J, et al** (2007) Interactions among PIN-  
669 FORMED and P-glycoprotein auxin transporters in *Arabidopsis*. *Plant Cell* **19**: 131–147

670 **Blilou I, Xu J, Wildwater M, Willemsen V, Paponov I, Friml J, Heidstra R, Aida M, Palme**

671 **K, Scheres B** (2005) The PIN auxin efflux facilitator network controls growth and  
672 patterning in Arabidopsis roots. *Nature* **433**: 39–44

673 **Brunoud G, Wells DM, Oliva M, Larrieu A, Mirabet V, Burrow AH, Beeckman T,**  
674 **Kepinski S, Traas J, Bennett MJ, et al** (2012) A novel sensor to map auxin response  
675 and distribution at high spatio-temporal resolution. *Nature* **482**: 103–106

676 **Chai S, Li E, Zhang Y, Li S** (2020) NRT1.1-Mediated Nitrate Suppression of Root Coiling  
677 Relies on PIN2- and AUX1-Mediated Auxin Transport. *Front Plant Sci* **11**: 1–12

678 **Chen RJ, Hilson P, Masson PH, Sedbrook J, Rosen E, Caspar T** (1998) The Arabidopsis  
679 thaliana AGRAVITROPIC 1 gene encodes a component of the polar-auxin-transport  
680 efflux carrier. *Proc Natl Acad Sci U S A* **95**: 15112–15117

681 **Fernandez R, Crabos A, Maillard M, Pradal C** (2022) High-throughput and automatic  
682 structural and developmental root phenotyping on Arabidopsis seedlings. *bioRxiv*  
683 2022.07.13.499903; doi: <https://doi.org/10.1101/2022.07.13.499903>

684 **Friml J, Wisniewska J, Benkova E, Mendgen K, Palme K** (2002) Lateral relocation of  
685 auxin efflux regulator PIN3 mediates tropism in ArabidopsisFriml, Jiří; Wiśniewska,  
686 Justyna; Benková, Eva; Mendgen, Kur Lateral relocation of auxin efflux regulator PIN3  
687 mediates tropism in Arabidopsis. *Lett to Nat* **415**: 1–4

688 **Giri J, Bhosale R, Huang G, Pandey BK, Parker H, Zappala S, Yang J, Dievart A,**  
689 **Bureau C, Ljung K, et al** (2018) Rice auxin influx carrier OsAUX1 facilitates root hair  
690 elongation in response to low external phosphate. *Nat Commun* **9**: 1–7

691 **Grones P, Abas M, Hajný J, Jones A, Waidmann S, Kleine-Vehn J, Friml J** (2018)  
692 PID/WAG-mediated phosphorylation of the Arabidopsis PIN3 auxin transporter  
693 mediates polarity switches during gravitropism. *Sci Rep* **8**: 1–11

694 **Huang F, Zago MK, Abas L, van Marion A, Galván-Ampudia CS, Offringa R** (2010)  
695 Phosphorylation of conserved PIN motifs directs Arabidopsis PIN1 polarity and auxin  
696 transport. *Plant Cell* **22**: 1129–1142

697 **Inahashi H, Shelley IJ, Yamauchi T, Nishiuchi S, Takahashi-Nosaka M, Matsunami M,**  
698 **Ogawa A, Noda Y, Inukai Y** (2018) OsPIN2, which encodes a member of the auxin  
699 efflux carrier proteins, is involved in root elongation growth and lateral root formation  
700 patterns via the regulation of auxin distribution in rice. *Physiol Plant* **164**: 216–225

701 **Dello Iorio R, Nakamura K, Moubayidin L, Perilli S, Taniguchi M, Morita MT, Aoyama T,**  
702 **Costantino P, Sabatini S** (2008) A genetic framework for the control of cell division  
703 and differentiation in the root meristem. *Science (80- )* **322**: 1380–1384

704 **Kiba T, Inaba J, Kudo T, Ueda N, Konishi M, Mitsuda N, Takiguchi Y, Kondou Y,**  
705 **Yoshizumi T, Ohme-Takagi M, et al** (2018) Repression of nitrogen starvation  
706 responses by members of the arabidopsis GARP-type transcription factor NIGT1/HRS1  
707 subfamily. *Plant Cell* **30**: 925–945

708 **Křeček P, Skůpa P, Libus J, Naramoto S, Tejos R, Friml J, Zažímalová E** (2009) Protein  
709 family review The PIN-FORMED ( PIN ) protein family of auxin transporters - Křeček et  
710 al. - 2009 - Genome Biology.pdf. GenomeBiology 1–11

711 **Krouk G, Lacombe B, Bielach A, Perrine-Walker F, Malinska K, Mounier E, Hoyerova  
712 K, Tillard P, Leon S, Ljung K, et al** (2010) Nitrate-regulated auxin transport by NRT1.1  
713 defines a mechanism for nutrient sensing in plants. Dev Cell **18**: 927–937

714 **Li C, Liu G, Geng X, He C, Quan T, Hayashi KI, De Smet I, Robert HS, Ding Z, Yang ZB**  
715 (2021) Local regulation of auxin transport in root-apex transition zone mediates  
716 aluminium-induced Arabidopsis root-growth inhibition. Plant J **108**: 55–66

717 **Liang G** (2022) Iron uptake, signaling, and sensing in plants. Plant Commun **3**: 100349

718 **Liao CY, Smet W, Brunoud G, Yoshida S, Vernoux T, Weijers D** (2015) Reporters for  
719 sensitive and quantitative measurement of auxin response. Nat Methods **12**: 207–210

720 **Liu D** (2021) Root developmental responses to phosphorus nutrition. J Integr Plant Biol **63**:  
721 1065–1090

722 **Liu H, Liu B, Chen X, Zhu H, Zou C, Men S** (2018) AUX1 acts upstream of PIN2 in  
723 regulating root gravitropism. Biochem Biophys Res Commun **507**: 433–436

724 **Luschnig C, Gaxiola RA, Grisafi P, Fink GR** (1998) EIR1, a root-specific protein involved  
725 in auxin transport, is required for gravitropism in Arabidopsis thaliana. Genes Dev **12**:  
726 2175–2187

727 **Müller A, Guan C, Gälweiler L, Tänzler P, Huijser P, Marchant P, Parry G, Bennett M,  
728 Wisman E, Palme K** (1998) AtPIN2 defines a locus of Arabidopsis for root gravitropism  
729 control. EMBO J **17**: 6903–6911

730 **Omelyanchuk NA, Kovrizhnykh V V., Oshchepkova EA, Pasternak T, Palme K,  
731 Mironova V V.** (2016) A detailed expression map of the PIN1 auxin transporter in  
732 Arabidopsis thaliana root. BMC Plant Biol **16**: 1–12

733 **Ottensschläger I, Wolff P, Wolverton C, Bhalerao RP, Sandberg G, Ishikawa H, Evans  
734 M, Palme K** (2003) Gravity-regulated differential auxin transport from columella to  
735 lateral root cap cells. Proc Natl Acad Sci U S A **100**: 2987–2991

736 **Petrášek J, Mravec J, Bouchard R, Blakeslee JJ, Abas M, Seifertová D, Wiśniewska J,  
737 Tadele Z, Kubeš M, Čovanová M, et al** (2006) PIN proteins perform a rate-limiting  
738 function in cellular auxin efflux. Science (80- ) **312**: 914–918

739 **Rahman A, Takahashi M, Shibasaki K, Wu S, Inaba T, Tsurumi S, Baskin TI** (2010)  
740 Gravitropism of Arabidopsis thaliana Roots Requires the Polarization of PIN2 toward  
741 the Root Tip in Meristematic Cortical Cells . Plant Cell **22**: 1762–1776

742 **Retzer K, Akhmanova M, Konstantinova N, Malínská K, Leitner J, Petrášek J, Luschnig  
743 C** (2019) Brassinosteroid signaling delimits root gravitropism via sorting of the  
744 Arabidopsis PIN2 auxin transporter. Nat Commun. doi: 10.1038/s41467-019-13543-1

745 **Retzer K, Lacek J, Skokan R, Del Genio CI, Vosolsobě S, Laňková M, Malínská K,**  
746 **Konstantinova N, Zažímalová E, Napier RM, et al** (2017) Evolutionary conserved  
747 cysteines function as cis-acting regulators of arabidopsis PIN-FORMED 2 distribution.  
748 *Int J Mol Sci.* doi: 10.3390/ijms18112274

749 **Ristova D, Kopriva S** (2022) Sulfur signaling and starvation response in Arabidopsis.  
750 *iScience* **25**: 104242

751 **Rosales MA, Mauel C, Nacry P** (2019) Abscisic Acid Coordinates Dose-dependent  
752 Developmental and Hydraulic Responses of Roots to Water Deficit. *Plant Physiol.* doi:  
753 10.1104/pp.18.01546

754 **Rouached H, Arpat AB, Poirier Y** (2010) Regulation of phosphate starvation responses in  
755 plants: Signaling players and cross-talks. *Mol Plant* **3**: 288–299

756 **Santelia D, Henrichs S, Vincenzetti V, Sauer M, Bigler L, Klein M, Bailly A, Lee Y, Friml**  
757 **J, Geisler M, et al** (2008) Flavonoids redirect PIN-mediated polar auxin fluxes during  
758 root gravitropic responses. *J Biol Chem* **283**: 31218–31226

759 **Sato EM, Hijazi H, Bennett MJ, Vissenberg K, Swarup R** (2015) New insights into root  
760 gravitropic signalling. *J Exp Bot* **66**: 2155–2165

761 **Sauer M, Kleine-Vehn J** (2019) PIN-FORMED and PIN-LIKES auxin transport facilitators.  
762 *Dev.* doi: 10.1242/dev.168088

763 **Singh M, Gupta A, Laxmi A** (2017) Striking the Right Chord: Signaling Enigma during Root  
764 Gravitropism. *Front Plant Sci* **8**: 1–17

765 **Su N, Zhu A, Tao X, Ding ZJ, Chang S, Ye F, Zhang Y, Zhao C, Chen Q, Wang J, et al**  
766 (2022) Structures and mechanisms of the Arabidopsis auxin transporter PIN3. *Nature.*  
767 doi: 10.1038/s41586-022-05142-w

768 **Swarup R, Kargul J, Marchant A, Zadik D, Rahman A, Mills R, Yemm A, May S,**  
769 **Williams L, Millner P, et al** (2004) Structure-function analysis of the presumptive  
770 Arabidopsis auxin permease AUX1. *Plant Cell* **16**: 3069–3083

771 **Swarup R, Kramer EM, Perry P, Knox K, Leyser HMO, Haseloff J, Beemster GTS,**  
772 **Bhalerao R, Bennett MJ** (2005) Root gravitropism requires lateral root cap and  
773 epidermal cells for transport and response to a mobile auxin signal. *Nat Cell Biol* **7**:  
774 1057–1065

775 **Ulmasov T, Murfett J, Hagen G, Guilfoyle T** (1997) Creation of a Highly Active Synthetic  
776 AuxRE. *Society* **9**: 1963–1971

777 **Ung KL, Winkler M, Schulz L, Kolb M, Janacek DP, Dedic E, Stokes DL, Hammes UZ,**  
778 **Pedersen BP** (2022) Structures and mechanism of the plant PIN-FORMED auxin  
779 transporter. *Nature.* doi: 10.1038/s41586-022-04883-y

780 **Utsuno K, Shikanai T, Yamada Y, Hashimoto T** (1998) AGR, an Agravitropic locus of  
781 Arabidopsis thaliana, encodes a novel membrane-protein family member. *Plant Cell*

782           Physiol **39**: 1111–1118

783 **Verslues PE, Agarwal M, Katiyar-Agarwal S, Zhu J, Zhu JK** (2006) Methods and  
784           concepts in quantifying resistance to drought, salt and freezing, abiotic stresses that  
785           affect plant water status. *Plant J* **45**: 523–539

786 **Vieten A, Vanneste S, Wiśniewska J, Benková E, Benjamins R, Beeckman T, Luschig**  
787           **C, Friml J** (2005) Functional redundancy of PIN proteins is accompanied by auxin-  
788           dependent cross-regulation of PIN expression. *Development* **132**: 4521–4531

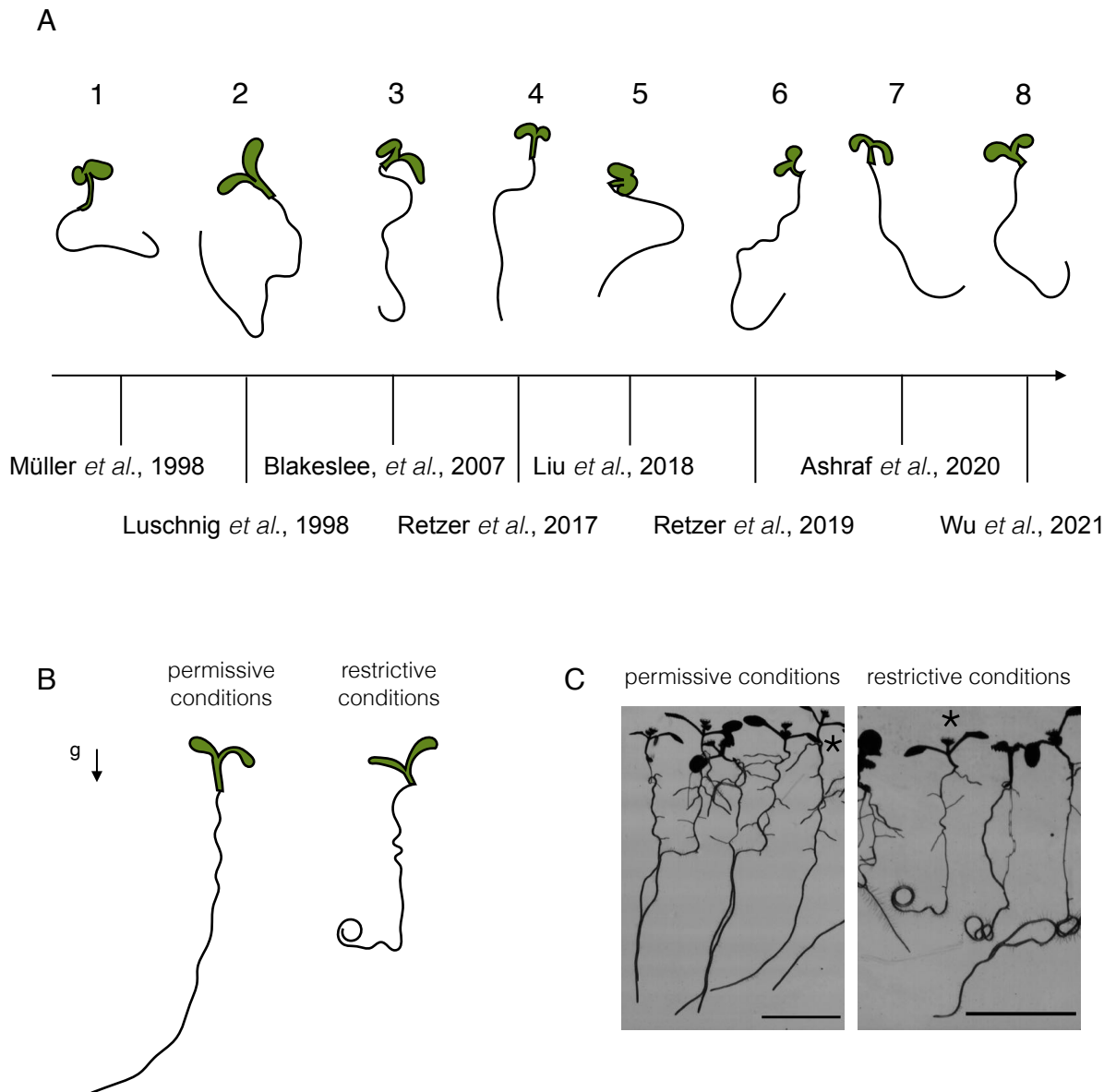
789 **Wu Y, Chang Y, Luo L, Tian W, Gong Q, Liu X** (2022) Abscisic acid employs NRP-  
790           dependent PIN2 vacuolar degradation to suppress auxin-mediated primary root  
791           elongation in *Arabidopsis*. *New Phytol* **233**: 297–312

792 **Xuan W, Beeckman T, Xu G** (2017) Plant nitrogen nutrition: sensing and signaling. *Curr*  
793           *Opin Plant Biol* **39**: 57–65

794 **Yang Z, Xia J, Hong J, Zhang C, Wei H, Ying W, Sun C, Sun L, Mao Y, Gao Y, et al**  
795           (2022) Structural insights into auxin recognition and efflux by *Arabidopsis* PIN1. *Nature*.  
796           doi: 10.1038/s41586-022-05143-9

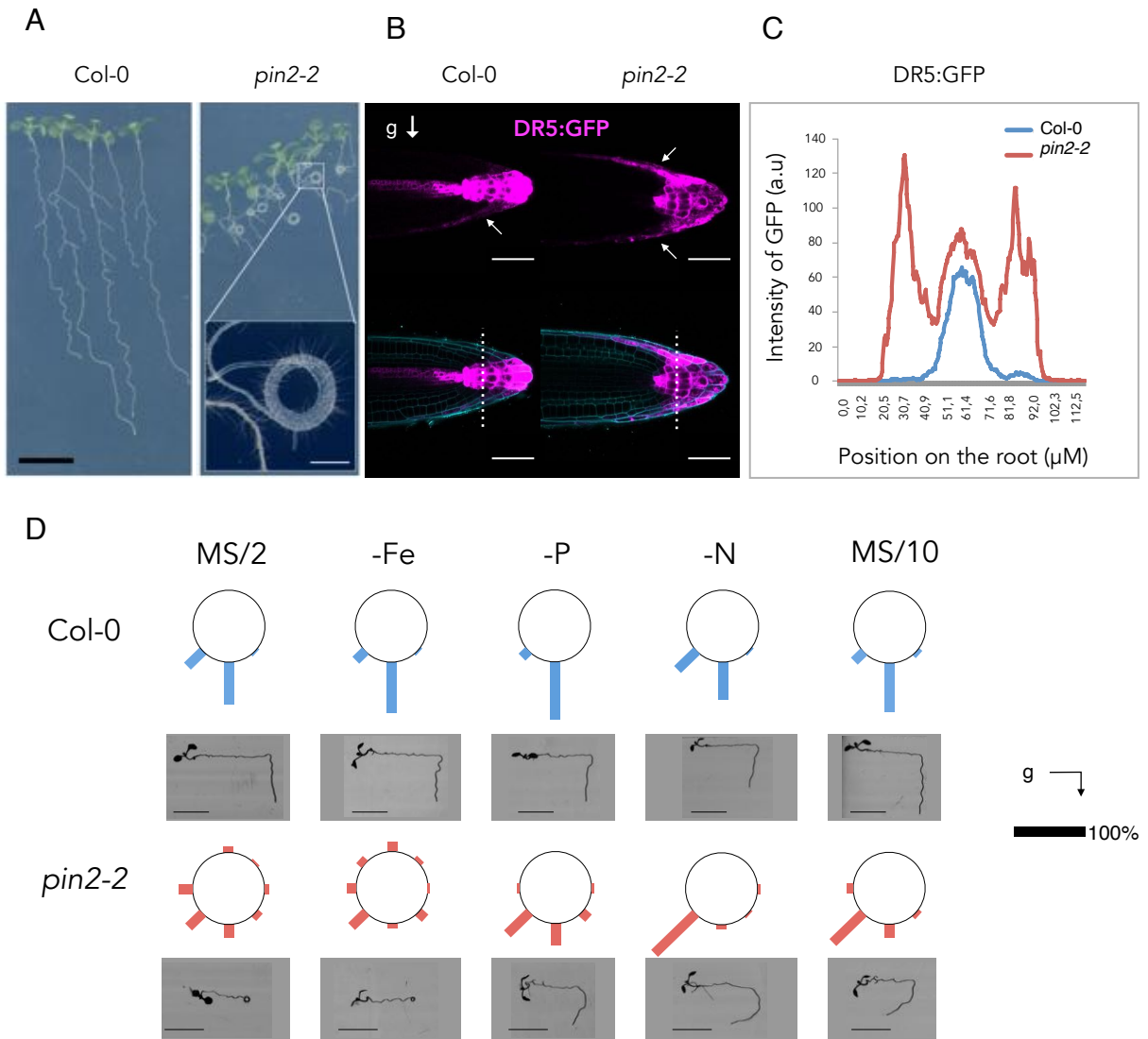
797

Figure 1.





**Figure 2.**



**Table 1.**


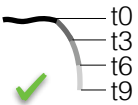

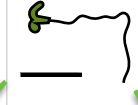
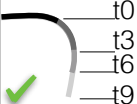
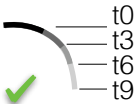


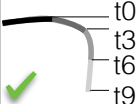
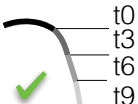
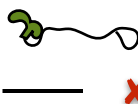
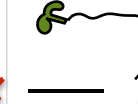
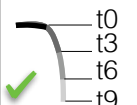


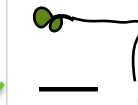
	Early gravitropism (9h)		Gravitropism (48h)		Growth (mm/24h)				
	restrictive conditions	permissive conditions	restrictive conditions	permissive conditions	restrictive conditions		permissive conditions		
	MS/2 , -Fe	-P , -N , MS/10	MS/2 , -Fe	-P , -N , MS/10	MS/2	- Fe	-P	-N	MS/10
Col-0					7,6 +/- 0,03	4,5 +/- 0,05	1,5 +/- 0,02	2,4 +/- 0,03	8,2 +/- 0,03
<i>pin1</i>					6,5 +/- 0,02	4,3 +/- 0,03	0,4 +/- 0,02	1,8 +/- 0,02	6,5 +/- 0,02
<i>pin2</i>					4,5 +/- 0,02	2,9 +/- 0,04	0,6 +/- 0,03	1,2 +/- 0,02	4,2 +/- 0,02
<i>pin3</i>					5,4 +/- 0,02	3,3 +/- 0,04	0,8 +/- 0,02	0,8 +/- 0,02	5,8 +/- 0,03

Figure 3.

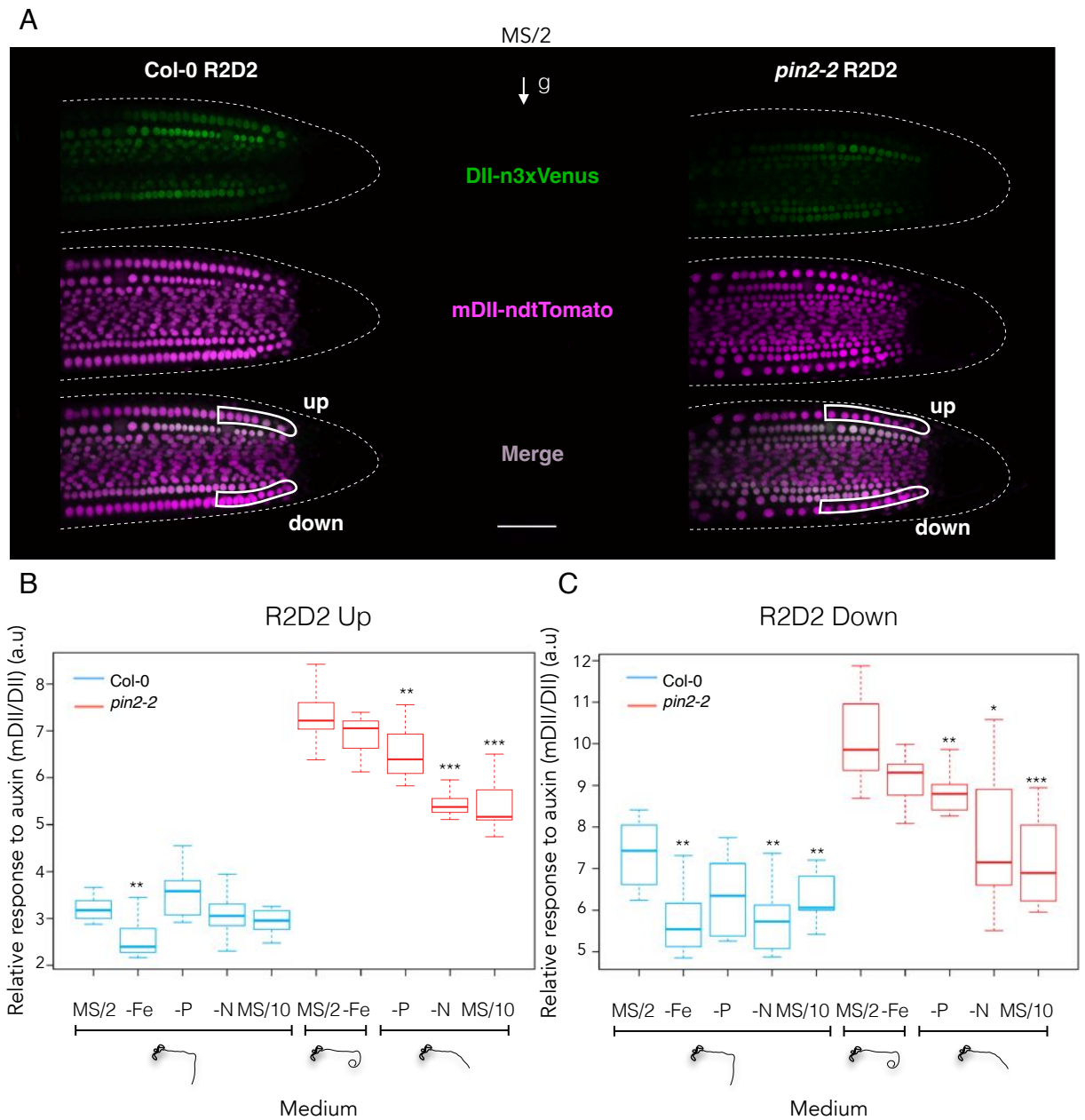
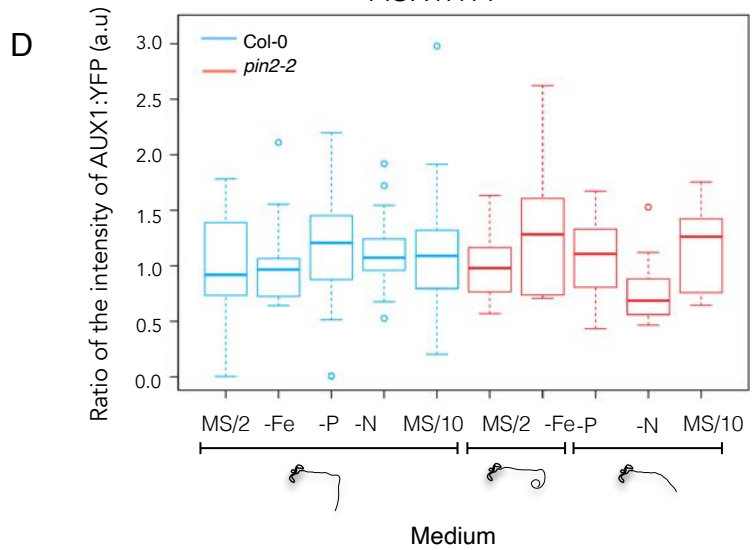
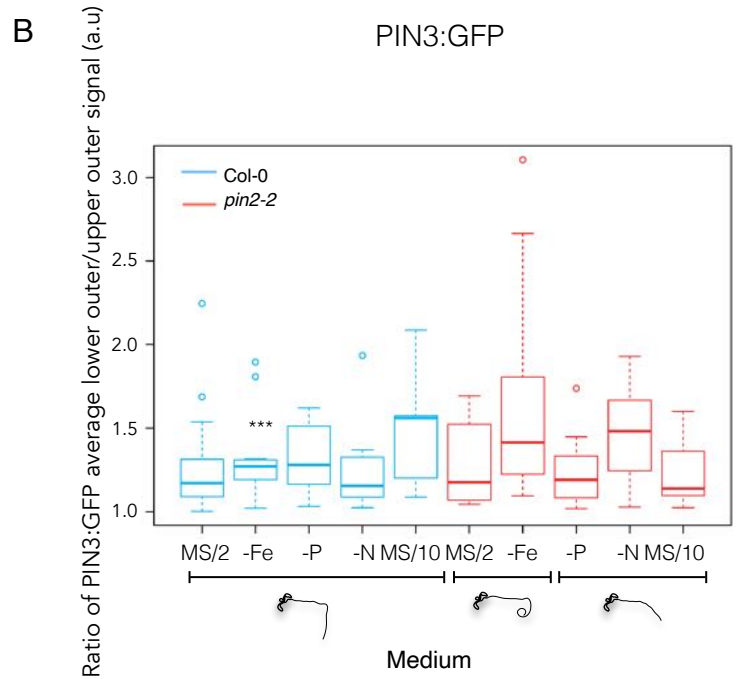
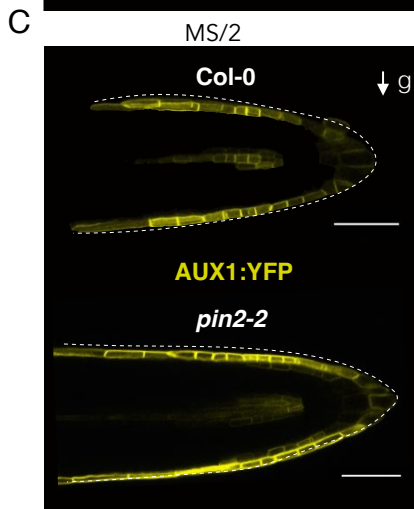
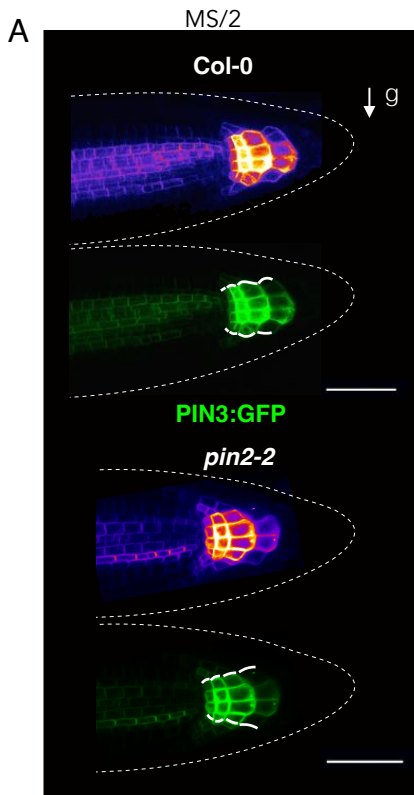


Figure 4.



**Figure 5.**

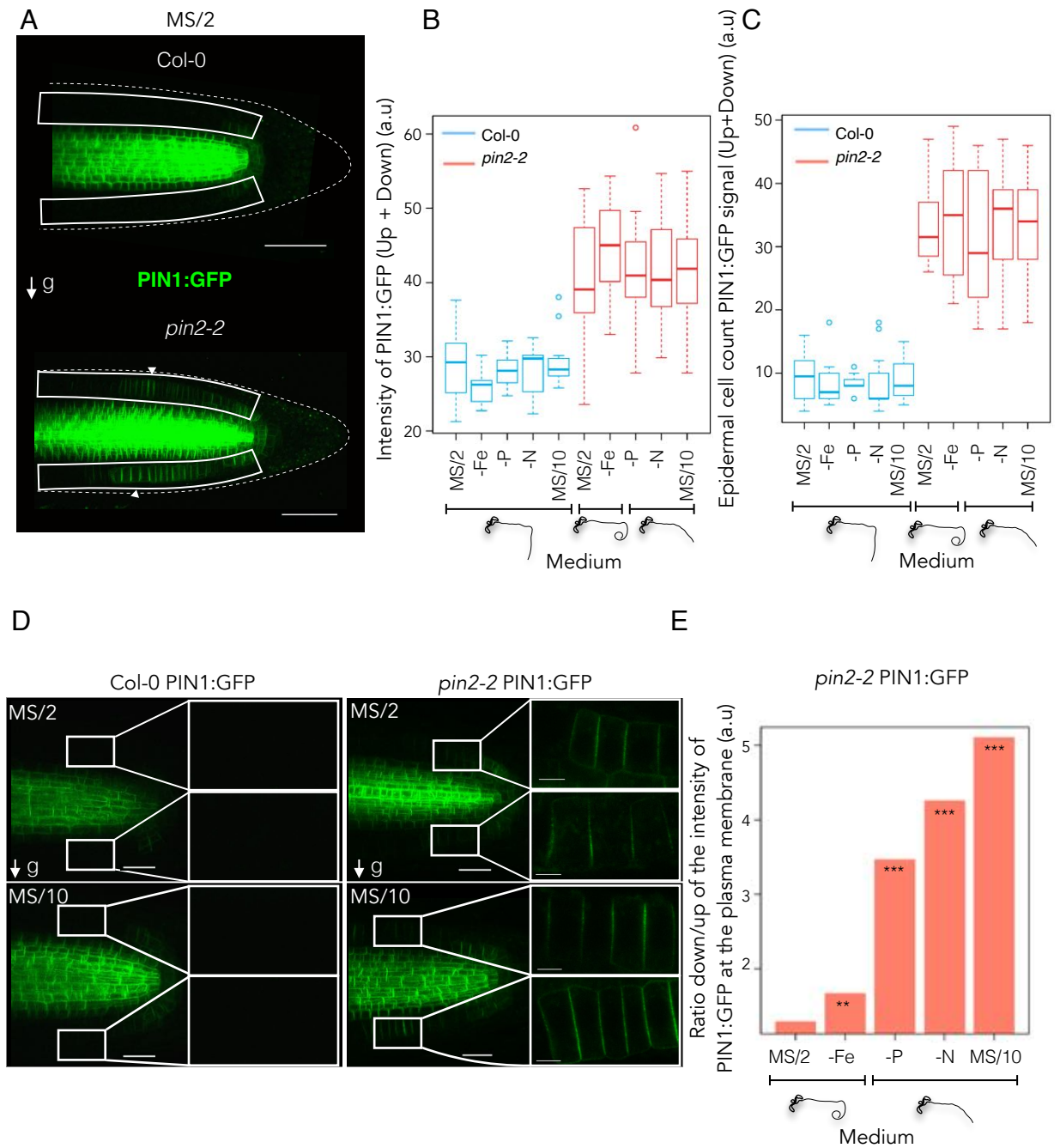


Figure 6.

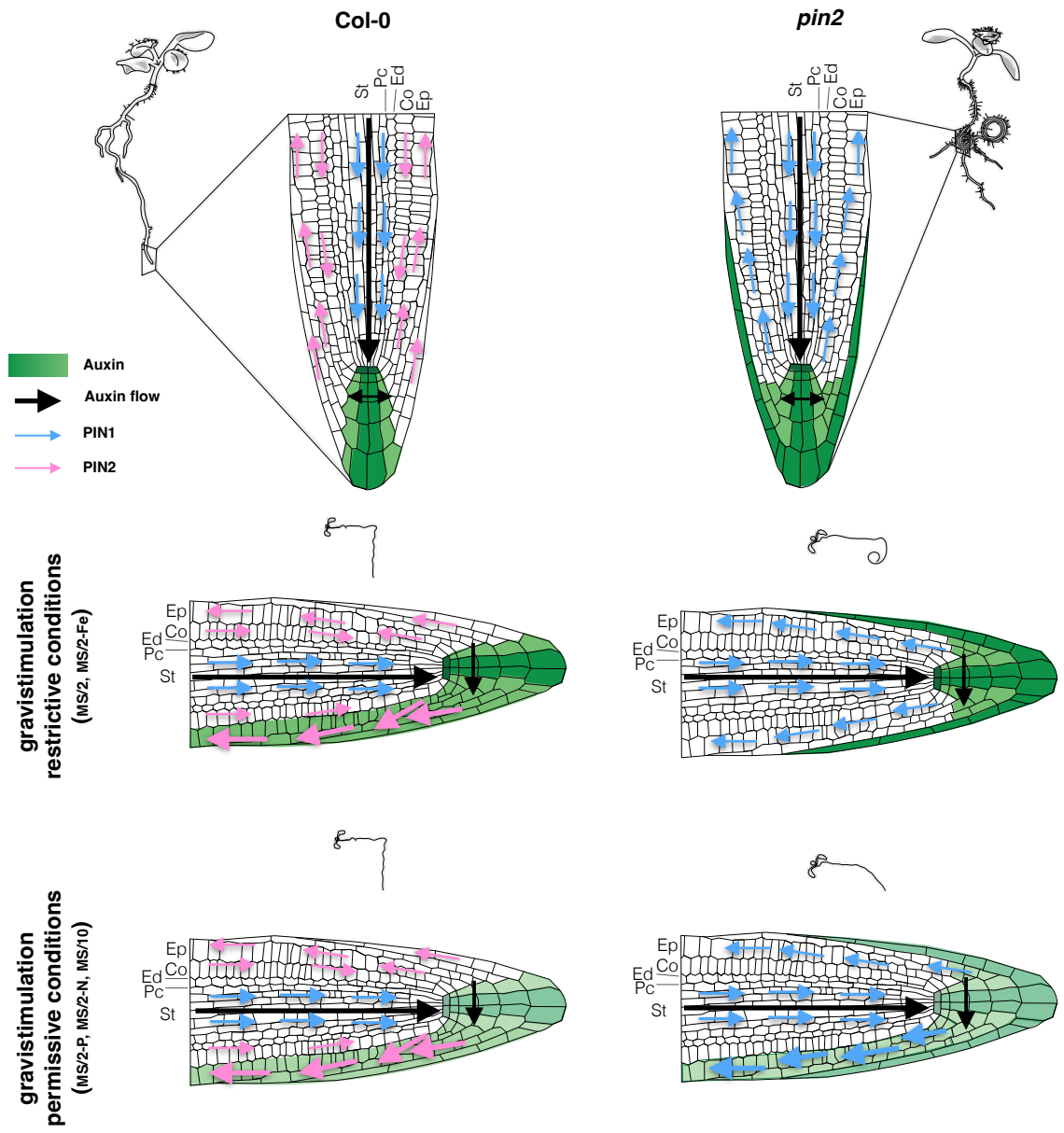
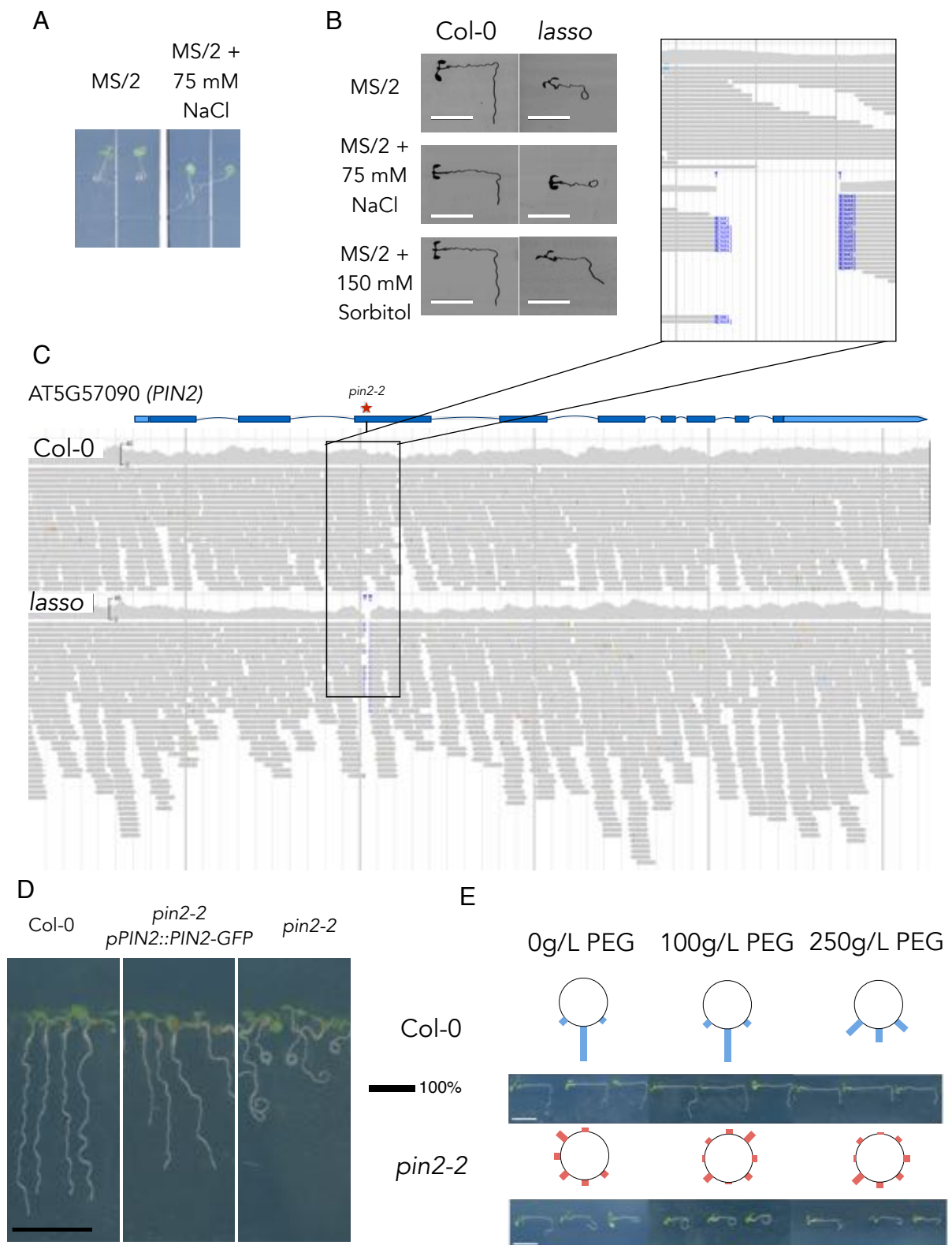
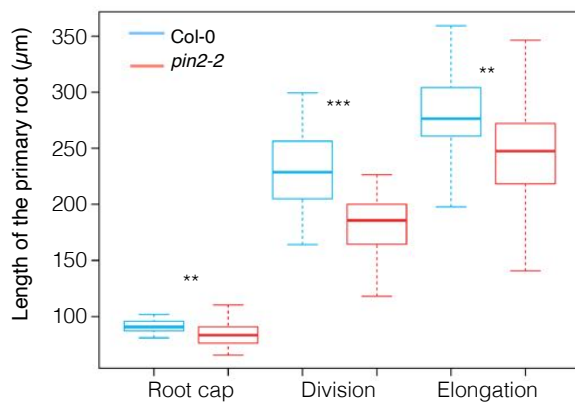


Figure S1.

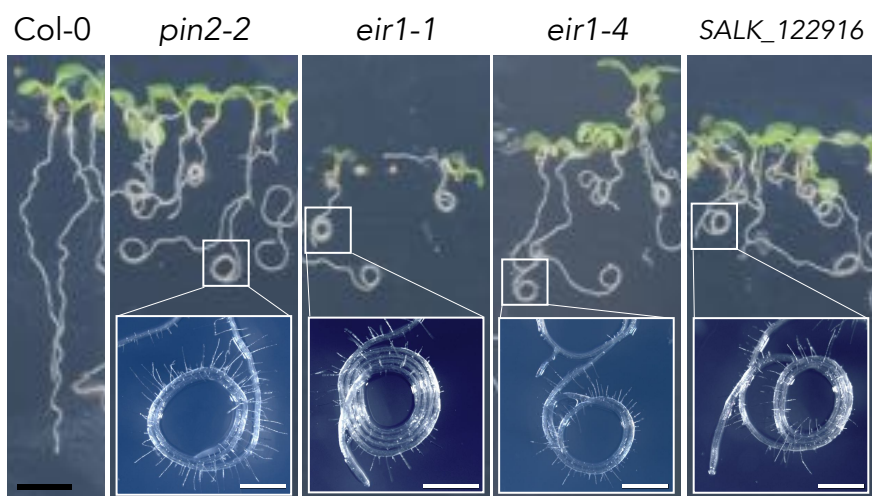


**Figure S2.**

**A**



**B**



**C**

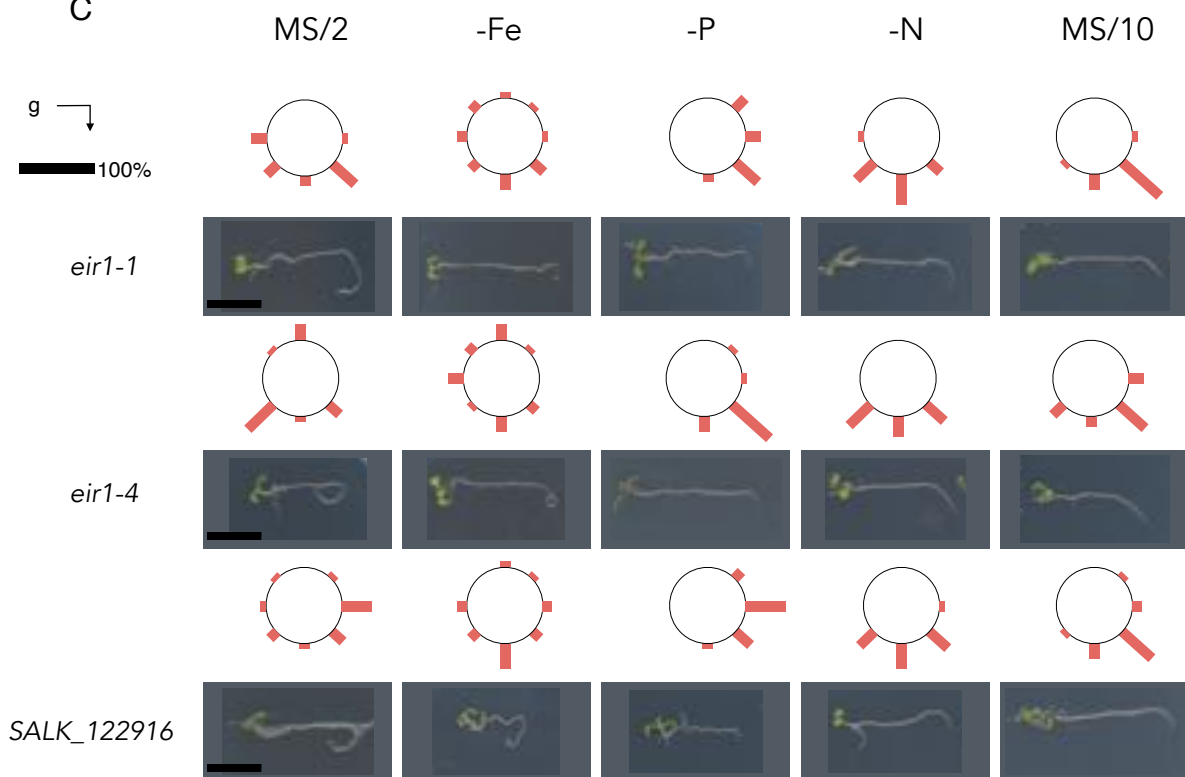
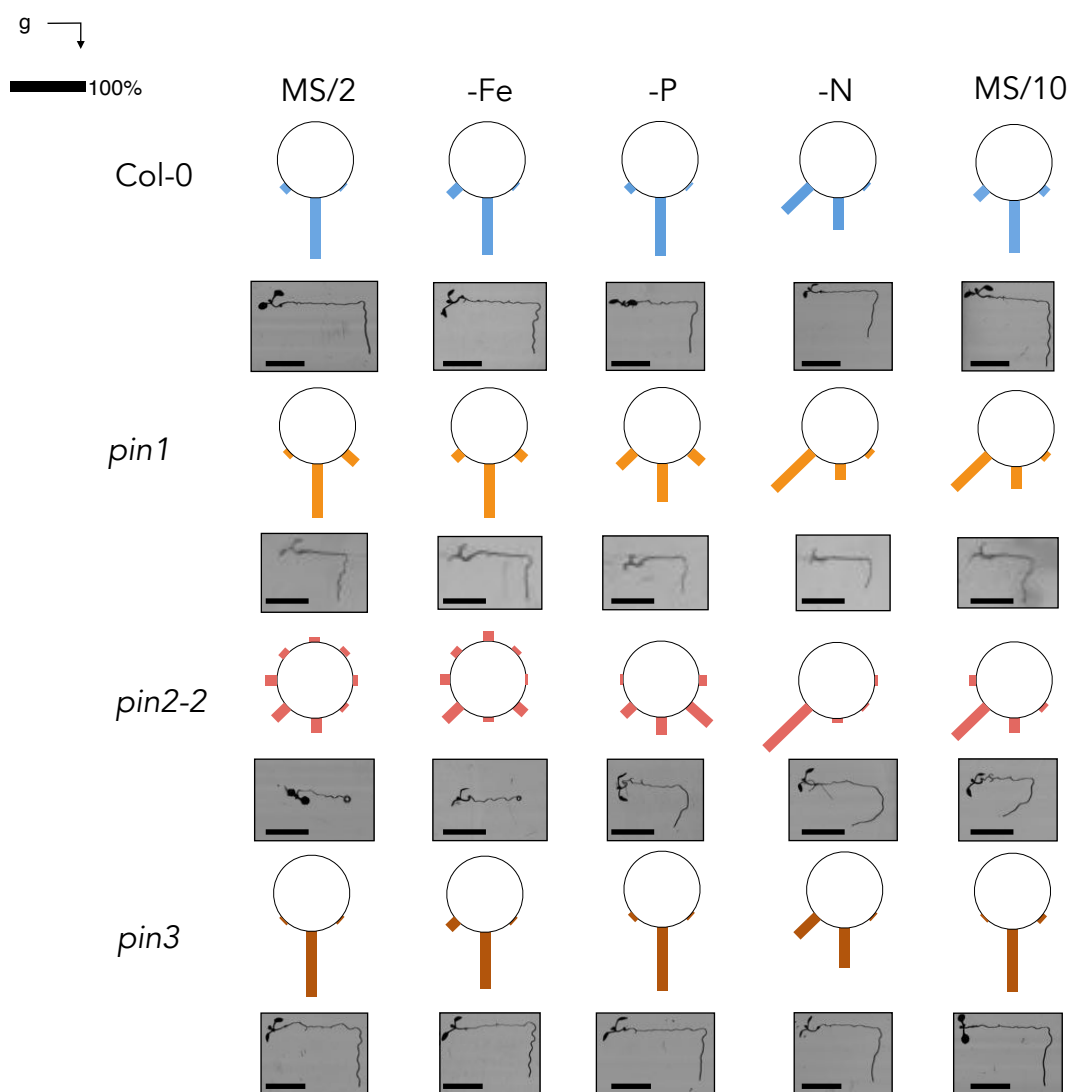




Figure S3.



**Figure S4.**

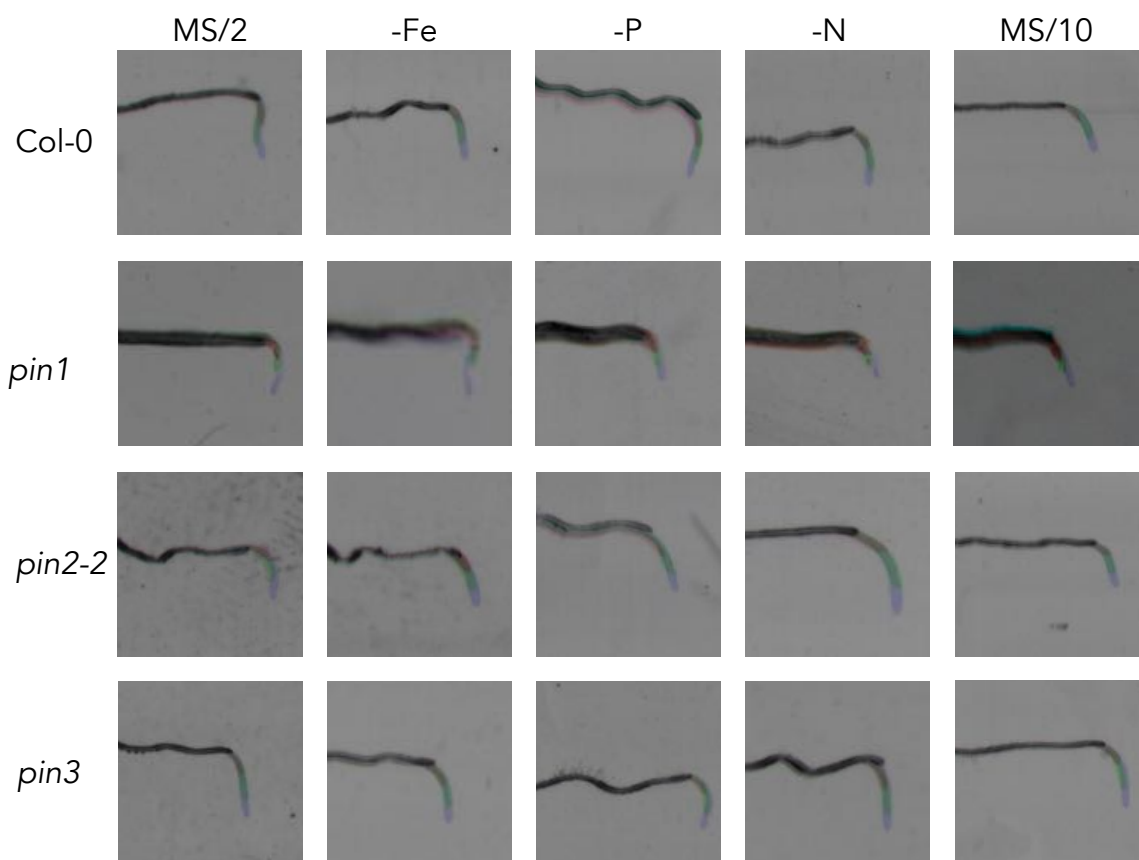


Figure S5.

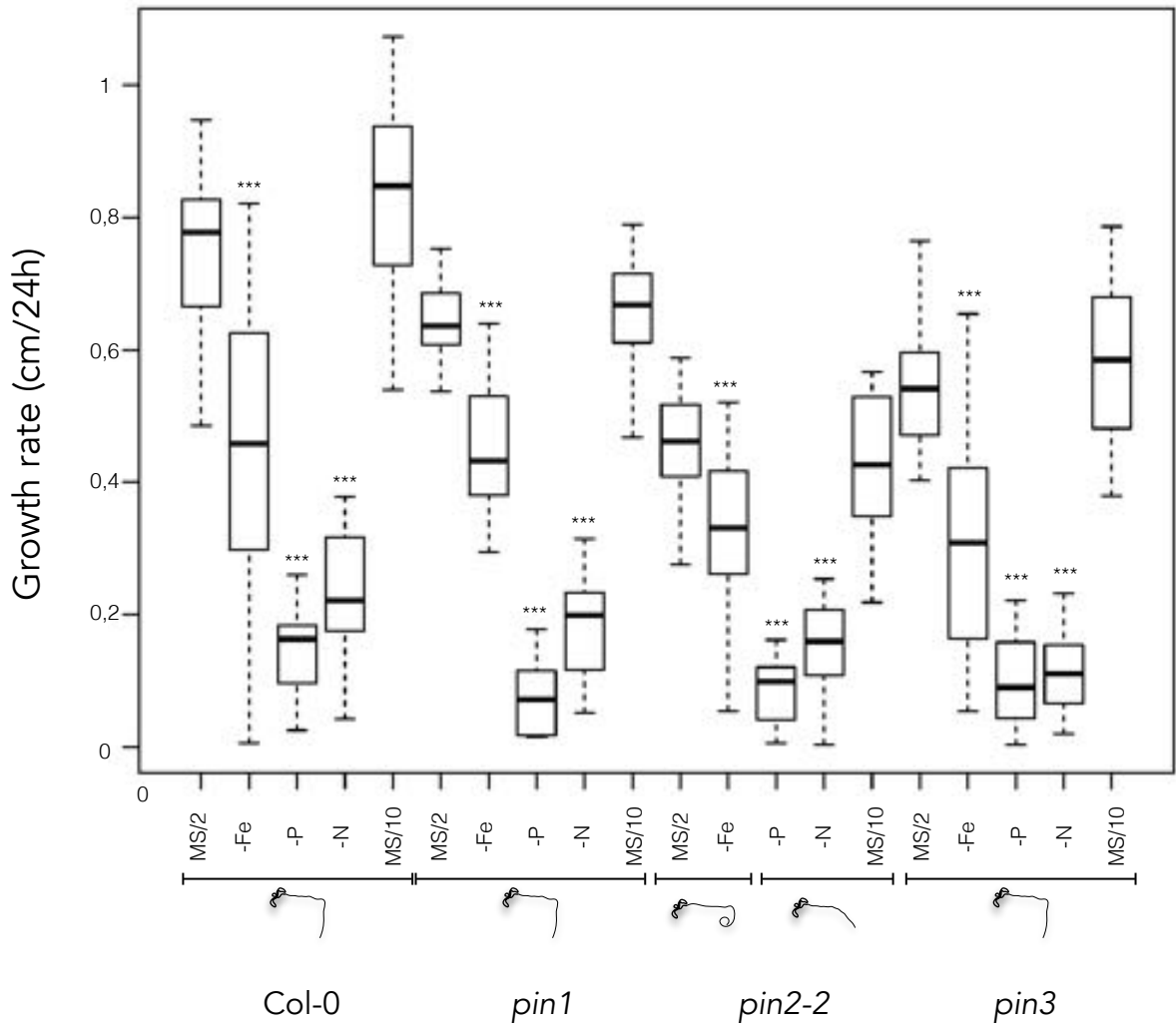


Figure S6.

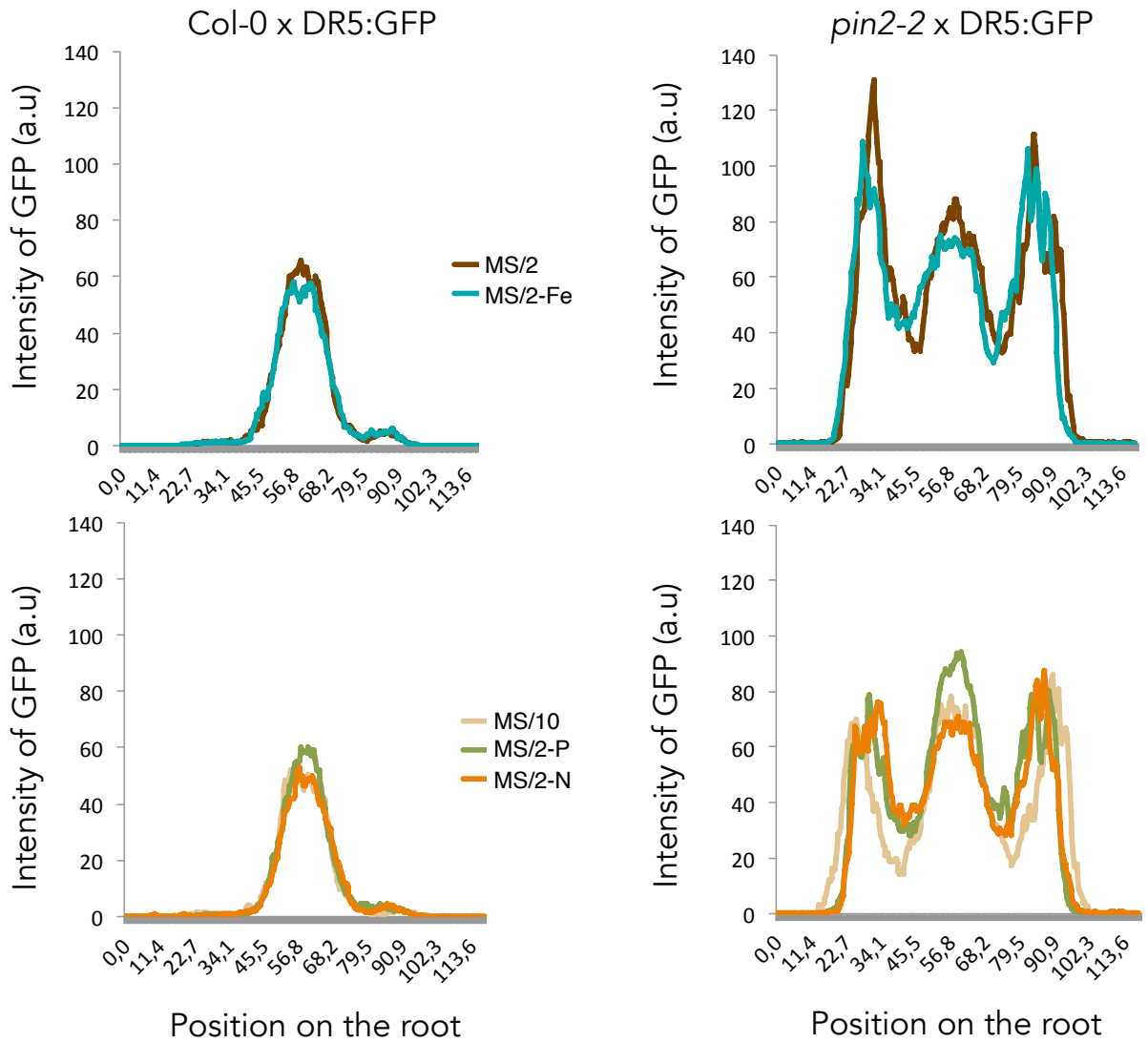
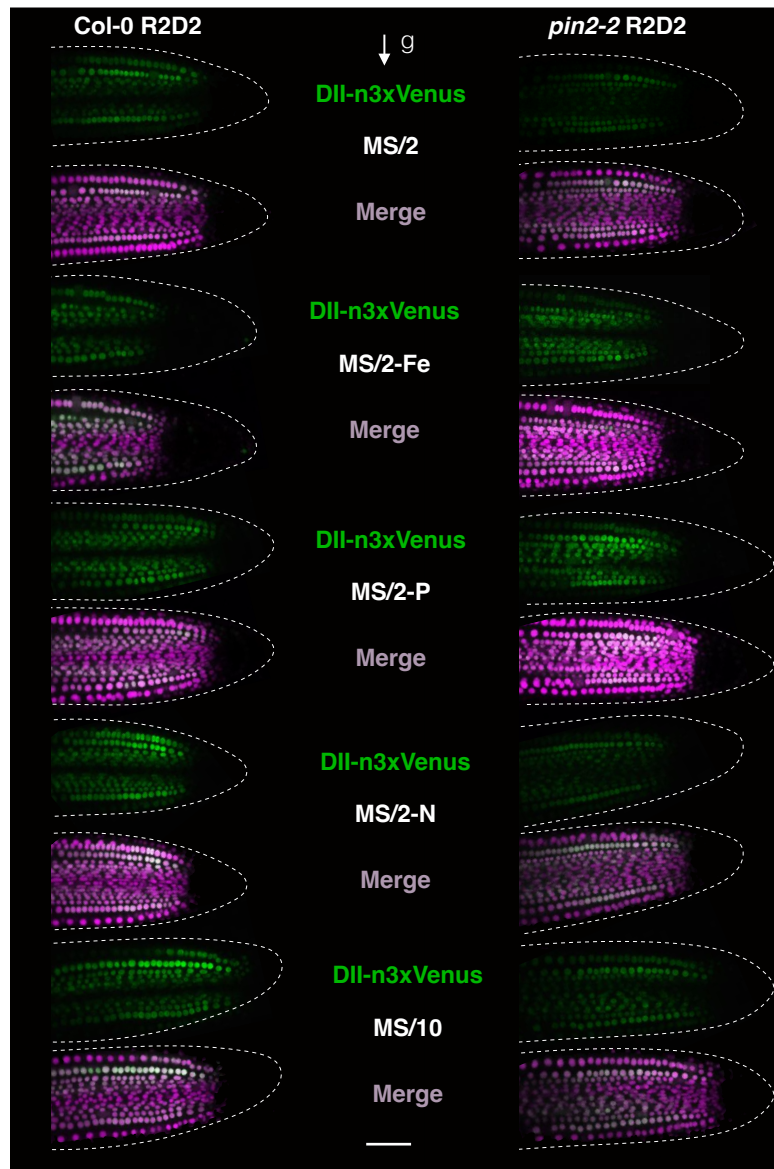


Figure S7.

A



R2D2 Ratio

B

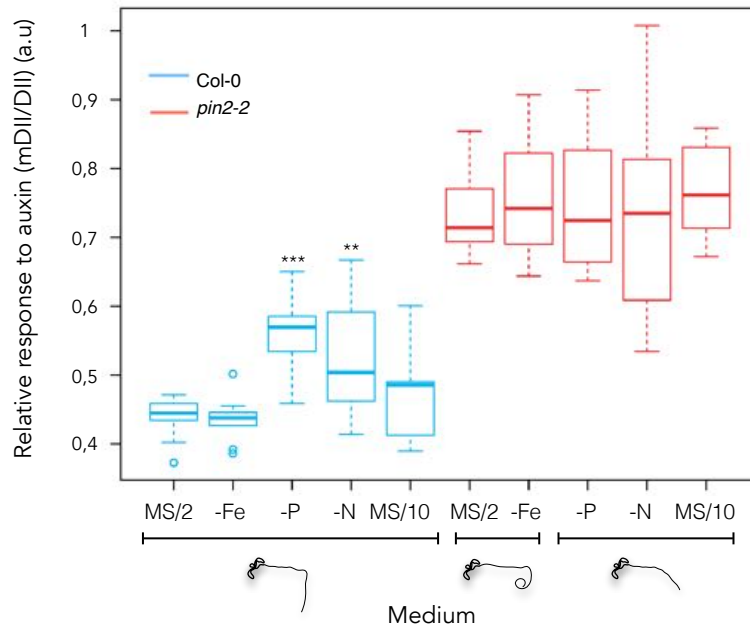


Figure S8.

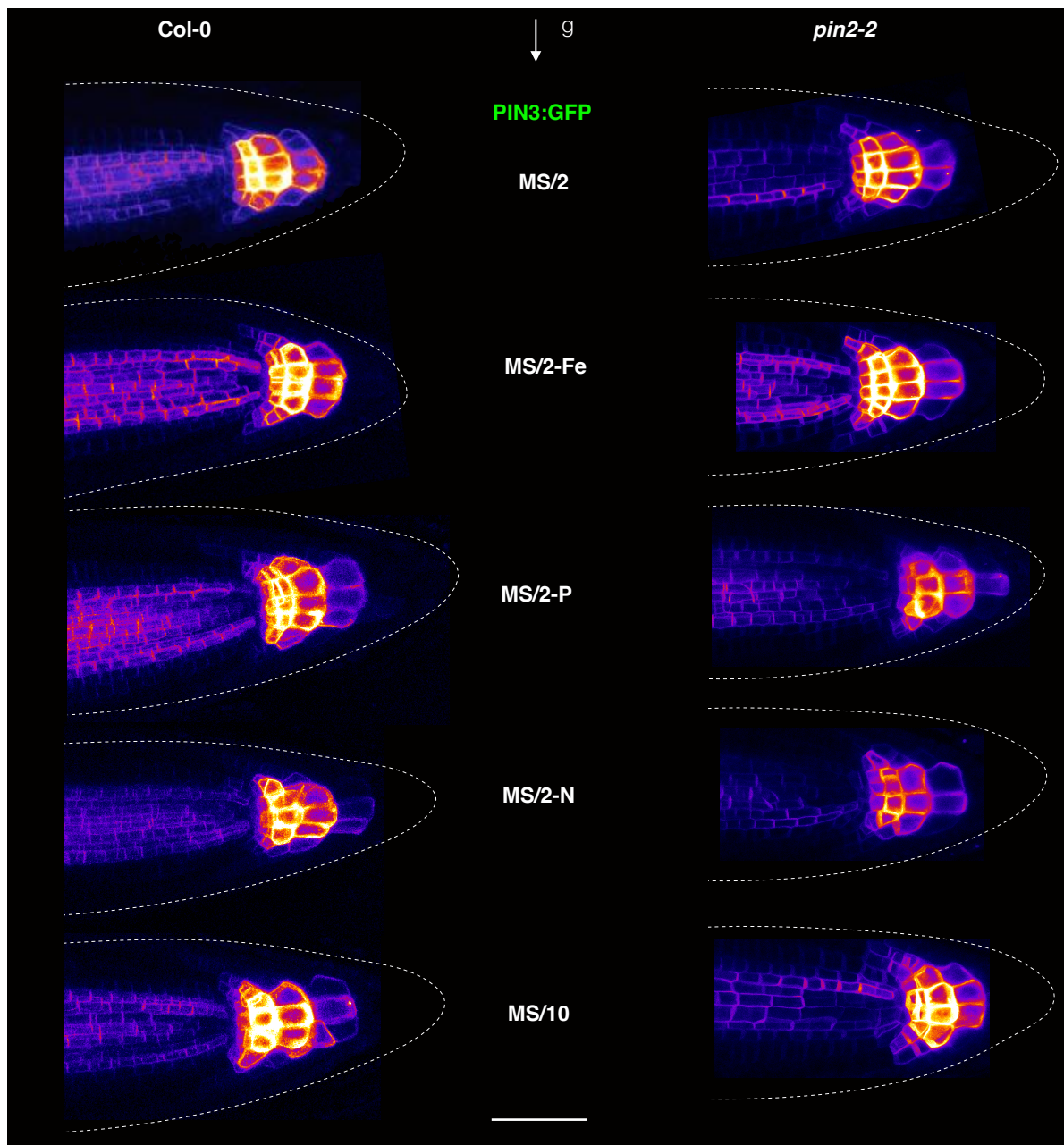


Figure S9.

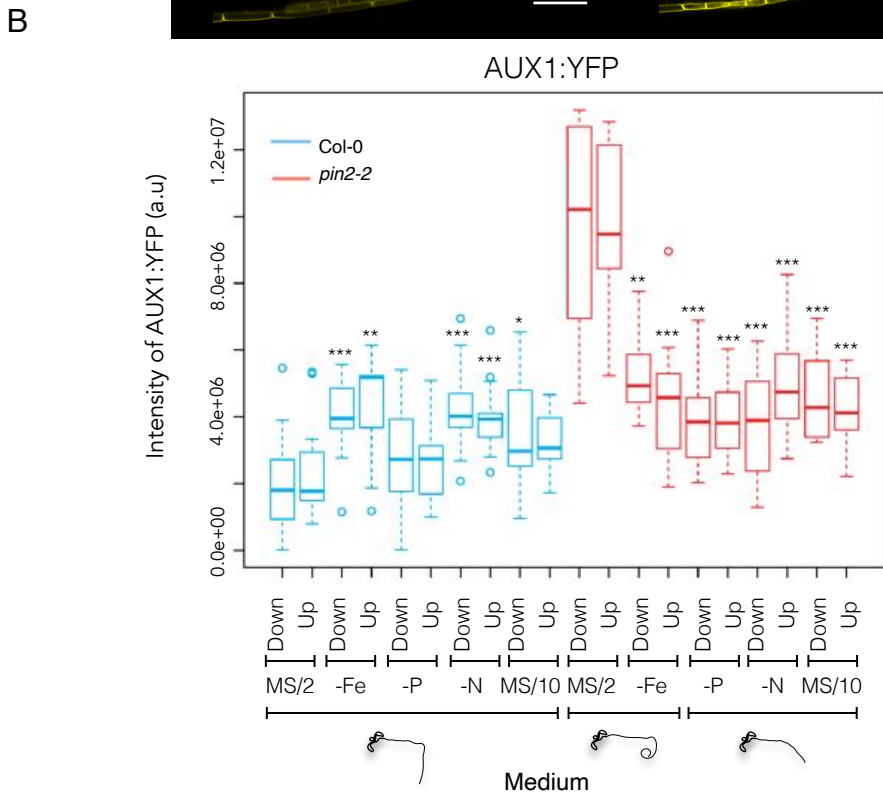
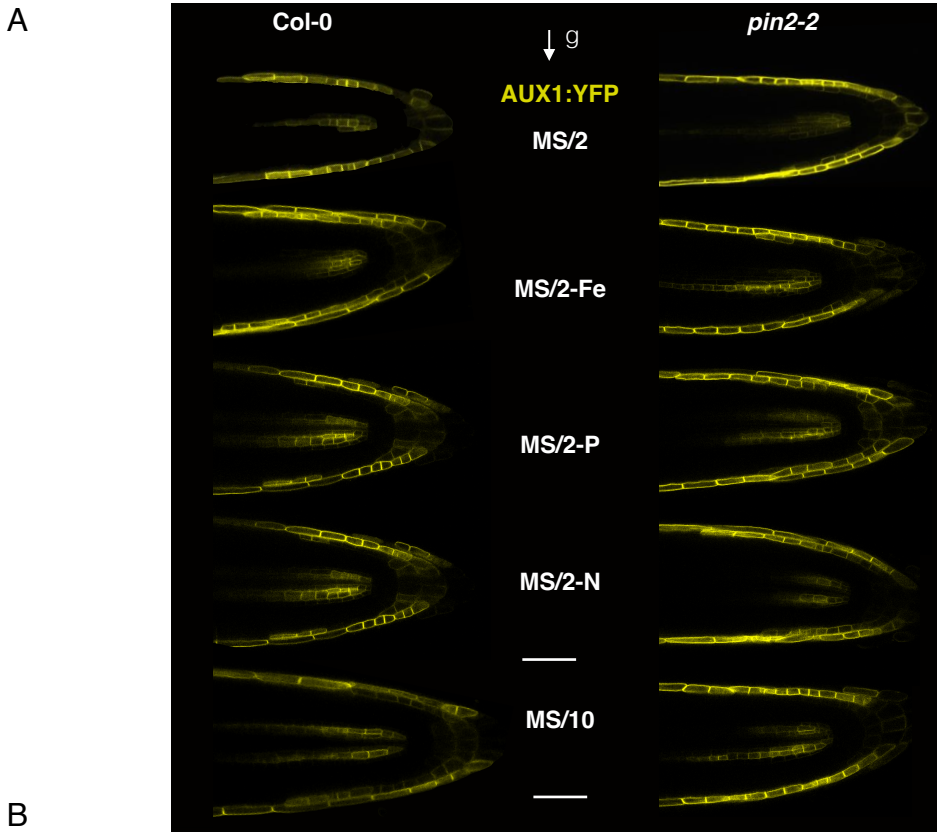


Figure S10.

